

# Electrokinetic mixing in microfluidic systems

Chih-Chang Chang · Ruey-Jen Yang

Received: 25 April 2007 / Accepted: 2 May 2007 / Published online: 5 June 2007  
© Springer-Verlag 2007

**Abstract** The applications of *electrokinetics* in the development of microfluidic devices have been widely attractive in the past decade. Electrokinetic devices generally require no external mechanical moving parts and can be made portable by replacing the power supply by small battery. Therefore, electrokinetic-based microfluidic systems can serve as a viable tool in creating a lab-on-a-chip (LOC) or micro-total analysis system ( $\mu$ TAS) for use in biological and chemical assays. Mixing of analytes and reagents is a critical step in realizing lab-on-a-chip. This step is difficult due to the low Reynolds numbers flows in microscale devices. Hence, various schemes to enhance micro-mixing have been proposed in the past years. This review reports recent developments in the micro-mixing schemes based on DC and AC electrokinetics, including electrowetting-on-dielectric (EWOD), dielectrophoresis (DEP), and electroosmosis (EO). These electrokinetic-based mixing approaches are generally categorized as either active or passive in nature. Active mixers either use time-dependent (AC or DC field switching) or time-independent (DC field) external electric fields to achieve mixing, while passive mixers achieve mixing in DC fields simply by virtue of their geometric topology and surface properties, or electrokinetic instability flows. Typically, chaotic mixing can be achieved in some ways and is helpful to mixing under large Péclet number regimes. The overview given in this article provides a potential user or researcher of electrokinetic-based technology to select the

most favorable mixing scheme for applications in the field of micro-total analysis systems.

**Keywords** Microfluidics · Electrokinetics · Micro-mixing · Lab-on-a-chip

## 1 Introduction

### 1.1 Microfluidic systems

Recent advances in the field of microelectronics have made possible the miniaturization of microfluidic systems on a microchip in order to carry out analytical analyses. Such a microfluidic system is generally known as a lab-on-a-chip or micro-total-analysis-system ( $\mu$ TAS). These systems perform a complete, integrated and automated analysis of the target analyte in a complex sample matrix. These devices offer significant advantages over their macro-scale counterparts, including a reduction in reagent consumption and the amount of chemical waste, a more rapid analysis, and a significant improvement in performance. The compact devices are portable and therefore allow samples to be analyzed on site rather than at a centralized laboratory. These devices are expected to have a low production cost and will be disposable after diagnostic use. A collection of topical reviews that discuss the history, design, application and future of lab-on-chip technologies, focusing on microfluidic flow devices, is published in Nature (Whitesides 2006; Janasek et al. 2006; Psaltis et al. 2006; Craighead 2006; deMello 2006; El-Ali et al. 2006; Yager et al. 2006).

In general,  $\mu$ TAS devices are designed to carry out the following functions: sample introduction, injection, mixing, reaction, dispensing, separation and detection through a series of micrometre-scale channels. Figure 1 presents a

---

C.-C. Chang · R.-J. Yang (✉)  
Department of Engineering Science,  
National Cheng Kung University,  
Tainan 70101, Taiwan  
e-mail: rjyang@mail.ncku.edu.tw

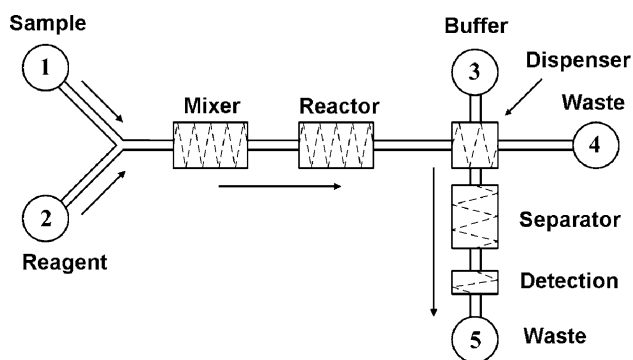


**Fig. 1** Illustration of microfluidic components in a typical lab-on-a-chip device

schematic illustration of a typical lab-on-a-chip. The sample of interest is introduced via port 1 and subsequently interacts with a reagent injected via port 2. The sample is then mixed with the reagent to facilitate the subsequent chemical reaction process. Finally, the reacted product is dispensed into a separation channel for component separation and detection using optical instrumentation. Forcing sources are required to manipulate fluids moving along the microchannels; mechanical force produced from syringe pumps is typical. Due to the large ratio of the surface area to volume in the microchannels, many interesting interfacial phenomena, namely wetting properties, surface tension, capillary effects, electrokinetic effects, etc. could be considered as driving forces. These effects are usually neglected in macro-scale fluid mechanics. Recent reviews on the micro-scale fluid mechanics were written by Stone et al. (2004) and Squires and Quakes (2005).

Microfluidic devices which employ electric fields to manipulate fluids demonstrate the most promise. Unlike using a syringe pump which needs to transport fluids through leaky connectors and must be hand connected, electrokinetic pumping simply embeds electrodes together with an inserted power supply within the devices. Also, electrokinetic pumping requires no external mechanical moving parts. Such systems can be made portable by replacing the power supply with a small battery. In fact, since mechanically driven parts are mostly bulky, many microfluidic related products which involve purely mechanically driven forces have almost become obsolete in the last few years (Chang 2006). Hence, we only focus on microfluidic systems which use electrokinetically driven forces in this article.

## 1.2 Electrokinetics

Electrokinetics generally involve the study of liquid or particle motion under the action of an electric field; this includes electroosmosis, electrophoresis, dielectrophoresis,

and electrowetting. In this review, we focus primarily on electroosmotic flow mixing. Regarding the information of electrophoresis, dielectrophoresis and electrowetting, interested readers can refer to many excellent references (e.g. Probstein 1994; Morgan and Green 2003; Jones 2005; Lee et al. 2002). Electroosmosis (EO) usually refers to the movement of electrolyte-containing fluid relative to a stationary charged surface (e.g. microchannel) by an applied electric field. Further, it is also classified into two subfields: classical (DC) electroosmosis and field-induced electroosmosis (or induced-charge electrokinetic phenomena) (Squires and Quakes 2005; Chang 2006).

Classical electroosmosis depends on surface charges at solid-liquid interfaces (Li 2004). These surface charges result from the surface functional groups. The surface charges attract counter-ions from the electrolyte solution and repel con-ions from the surface to maintain local electroneutrality. An excess of charge is built up near the solid-liquid interface, thus forming an electrical double layer (EDL) with a thickness equal to the Debye screening length ( $\lambda_D$ ) (Hunter 1981); this results in a screened electric field normal to the surface ( $E_s$ ). Its strength depends on its surface charge density. The double layer thickness is approximately 10–100 nm and corresponds to the electrolyte solution (e.g. KCl solution) with a bulk concentration of  $10^{-3}$  to  $10^{-5}$  M. The counter-ions screen the electric field ( $E_s$ ) such that it rapidly decays from  $E_s$  to zero over the distance of  $\lambda_D$ . The potential drop over this distance is known as the zeta potential ( $\zeta$ ), which is dependent on the surface charge density and Debye screening length. The surface charge density is usually dependent on the pH value, bulk concentration of electrolytes and surface material (Hunter 1981). For most materials of microchannels with moderate surface charge density in typical electrolyte solutions, the magnitude of the zeta potential is less than 100 mV. When an external electric field is applied parallel to the channel wall ( $E_{\parallel}$ ), an electrical force within the thin electrical double layer is produced which drives the mobile ions in this double layer. Due to fluid viscosity, fluid surrounding the ions will move along. Since there is an excess of counter-ions and a net momentum transfer to the fluid, bulk fluid motion is produced. The resulting flow field has a high shear rate within the thin double layer; the velocity outside of this layer is known as the Smoluchowski slip velocity (Probstein 1994):

$$u_s = -\frac{\varepsilon_f \zeta}{\mu} E_{\parallel}, \quad (1)$$

where  $\varepsilon_f$  and  $\mu$  are the permittivity and viscosity of the fluid. Equation (1) indicates that electroosmotic flow velocity is linearly proportional to the external electric field which is labeled as linear electroosmosis. When the double

layer thickness is much smaller than the channel dimension, electroosmotic flow is the same as the wall-driven flow, resulting in a plug-like velocity profile.

In field-induced electroosmosis, double layer polarization near the solid–liquid interface is primarily due to surface charges induced by the external electric field but not the permanent surface charges of the channel surface. The inducing surface in the literature is either the electrode itself (Ramos et al. 1999; Green et al. 2000; Gonzalez et al. 2000; Lastochkin et al. 2004) or is independent of electrodes e.g. dielectric surface (Thamida and Chang 2002), a conducting ion-exchange granular (Dukhin 1991; Ben and Chang 2002), a conducting surface (Squires and Bazant 2004), etc. The former generally requires an AC electric field with a suitable frequency and is labeled as “AC electroosmosis” (Ramos et al. 1999; Morgan and Green 2003). The latter can occur as either DC or AC electric fields. The field-induced zeta potential is usually dependent on the external electric field strength ( $E$ ). In this case, the electroosmotic slip velocity would be proportional to the square of the external electric field (i.e.  $u_s \sim E^2$ ) (Dukhin 1991; Mishchuk and Takhistov 1995; Ben and Chang 2002; Squires and Bazant 2004). Thus, it is also known as nonlinear electroosmosis in the literature. This nonlinear slip velocity is often much larger than the Smoluchowski slip velocity shown in Eq. (1). This would be beneficial for high-throughput electrokinetic-based microfluidic systems with low applied voltages (Chang 2006).

### 1.3 Microfluidic mixing and mixing principles

The mixing of two or more miscible fluids in microfluidic systems is important in a variety of applications, e.g. to achieve a homogenized solution of the reagents to ensure maximum products in chemical reactions. Furthermore, biological processes such as cell activation, enzyme reactions and protein folding commonly involve reactions which require the mixing of reactants for initiation and fast processing. An ideal micromixer should possess features of rapid and efficient mixing, be compact in size, be easily integrated with other components. Achieving such a mixer is an essential but challenging task when developing microfluidic devices for chemical and biological analysis applications. The development of micromixing approaches for microfluidic applications has attracted the attention of many research groups worldwide, and a quite large number of papers have already appeared which reported on the development of micromixers based on different strategies (Nguyen and Wu 2005; Hessel et al. 2005; Hardt et al. 2005).

Since viscous forces dominate the flow in microfluidic devices and the flow is limited to the low Reynolds number regime, turbulence does not readily occur. In electroki-

netically driven flow in microfluidic systems, the Reynolds number is typically less than unity (i.e. Stokes flow). In a conventional straight microchannel, the Stokes flow is generally unidirectional. Even in curved or twisted channels (Chen et al. 2006), the transverse flow component (i.e. the secondary flow) is very small compared to the streamwise component since the inertial effect is very weak. Therefore, mixing of two fluid streams within the microchannel chiefly takes place as the result of molecular diffusion. The rate of diffusive mixing in microscale channels is very slow compared to the convection of the fluid along the channel since the Péclet number ( $Pe = Uw/D$ , where  $U$  is the average flow velocity,  $w$  is the channel dimension, and  $D$  is the molecular diffusivity) of typical microchannel flows is very high. The diffusive mixing time is given by  $t_D \sim w^2/D$  and the mixing length ( $L_m$ ) along the downstream channel increases linearly with the Péclet number (i.e.  $L_m \sim Pe \times w$ ). In practice, many biochemical applications, e.g. immunoassays and DNA hybridization, require the rapid mixing of macromolecules with relatively low molecular diffusivity (e.g.  $10^{-11} \text{ m}^2/\text{s}$  for DNA and small proteins). Typical values in conventional straight microchannel devices show an average electroosmotic flow velocity of  $500 \mu\text{m/s}$  and a channel dimension of  $100 \mu\text{m}$ ; the mixing time and mixing length required to achieve a complete mixing are approximately  $1,000 \text{ s}$  and  $0.5 \text{ m}$ , respectively. However, these values are unsuitable for rapid biochemical analysis in  $\mu\text{TAS}$  devices. Accordingly, developing the means to enhance mixing in micro-scale devices is essential. To reduce these values, the diffusion length ( $w$ ) must be shortened and the interfacial contact area should be increased within the microchannel. A large interfacial contact area allows for a large area of mass transfer, while a shortened diffusion length increases the concentration gradients and increases the mass flux. In general, chaotic mixing is a powerful way to reduce the diffusion length and increase the interfacial contact area (Ottino 1989; Wiggins and Ottino 2004).

Although it is difficult to induce turbulence (so-called Eulerian chaos) in microchannels, an effective mixing in low Reynolds number flow regimes can be obtained by the chaotic advection mechanism (or so-called Lagrangian chaos or laminar chaos). This mixing can occur in regular “smooth” (from a Eulerian viewpoint) flows and provides an effective increase in the interfacial contact area and concentration gradient due to reduction of the striation thickness (i.e. diffusion length) (Ottino 1989; Wiggins and Ottino 2004). In this way, mixing time and length can be considerably reduced. If an exponential reduction of striation thickness should occur, the mixing time and mixing length can be reduced down to  $t_m \sim \ln(Pe)$  and  $L_m \sim \ln(Pe)$ , respectively, for chaotic flows in the limit of large  $Pe$  (Stroock et al. 2002a; Ottino and

Wiggins 2004a; Song et al. 2003). It is important to note that chaotic advection cannot occur in steady two-dimensional flows, but is restricted to two-dimensional time dependent flows and three-dimensional flows. From this principle, we can immediately conclude that a small cylindrical rotor spinning around its centre with a uniform angular frequency (i.e. Couette flow) is not likely to be an efficient micromixer, while two such rotors turned on and off alternatively (a blinking vortex model) can form an efficient mixer (Ottino 1989). In Couette flow, the fluid is only stretched and chaotic advection cannot be induced, therefore the mixing is poor. In contrast, when two alternating rotors are arranged together, the fluid is repeatedly stretched around one of them and then folded around the other; hence, chaotic advection can be induced and then the mixing is good. Consequently, effective mixing always requires repeated stretching and folding of fluid elements. Blinking vortex models are similar to the link twist map (LTM) strategy which is based on a dynamic system theory described in the literature (Wiggins and Ottino 2004; Ottino and Wiggins 2004b). An LTM is often obtained when the dynamic system has a structure such that the motion can be described by the repeated application of two twist maps. Over the past few years, many effective micromixers have been designed according to the LTM strategy (Wiggins and Ottino 2004).

As discussed above, mixing in microfluidic channels relies primarily on molecular diffusion or chaotic advection (laminar chaos) mechanisms. The diffusive mixing effect

can be improved by increasing the interfacial contact area between the different fluids and reducing the diffusion length between them. This paper reviews various strategies to improve the mixing of two or more fluids in microchannels based on electrokinetics.

## 2 Basic methodology

As shown in Fig. 2, either theoretical or experimental approaches were adopted to study micromixing in the literature. Many electrokinetic micromixers are made of dielectric materials such as silicon, glass, polymers, etc. Within the framework of the continuum assumption, the electrokinetic flow in micromixers can be modeled by the continuity equation as well as the momentum equation, modified to include the electrical body force term ( $\mathbf{F}$ ). These are given respectively by

$$\nabla \cdot \mathbf{u} = 0 \quad (2)$$

and

$$\rho_f \left( \frac{\partial \mathbf{u}}{\partial t} + \mathbf{u} \cdot \nabla \mathbf{u} \right) = -\nabla p + \mu \nabla^2 \mathbf{u} + \mathbf{F}, \quad (3)$$

where  $t, \mathbf{u}, p, \rho_f$  and  $\mu$  are time, fluid velocity, pressure, fluid density and viscosity, respectively.  $\mathbf{F}$  is the Coulombic force ( $\rho_e \mathbf{E}$ ) arising due to the presence of free space charge  $\rho_e$  interacting with  $\mathbf{E}$ , where  $\rho_e$  is the net free charge density in the bulk liquid at the solid-liquid interface (i.e.

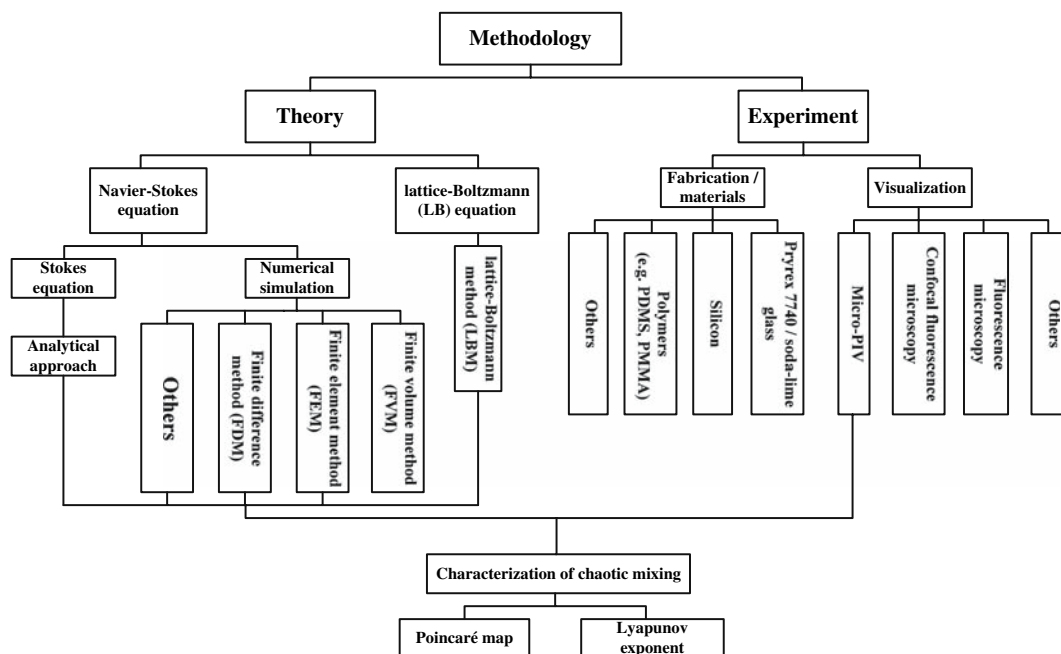


Fig. 2 Methodology classifications for the study of micro-mixing

EDL) and  $\mathbf{E}$  is the externally applied DC or AC electric field. In general, the distribution of net free charge density is described by the Poisson–Nernst–Planck model (Probstein 1994; Li 2004). Under conditions of thermodynamic equilibrium, the ion concentration in EDL is described by the Boltzmann distribution and the net free charge density can be simply described by the Poisson–Boltzmann equation (Hunter 1981). Furthermore, the electrical driving force term in Eq. (3) can be assumed to be neglected when the EDL thickness is much smaller than channel dimension and no free net charge density exists in the bulk liquid. The effect of electroosmotic flow is considered to be the slip wall boundary condition shown in Eq. (1). In the literature, Eqs. (2) and (3) were usually solved through various well-known numerical methods such as the finite difference method (FDM), finite volume method (FVM), and finite element method (FEM).

For typical microfluidic applications, the Reynolds number is much less than unity ( $Re = \rho_f U w / \mu \ll 1$ ) and the flow can be approximated as a creeping flow (i.e. Stokes flow). Then, the convection term in Eq. (3) can be neglected, and thus the electrokinetic flow in micro-devices is governed by Eqs. (2) and (4):

$$\rho_f \frac{\partial \mathbf{u}}{\partial t} = -\nabla p + \mu \nabla^2 \mathbf{u} + \mathbf{F}. \quad (4)$$

In addition, if the time required to reach the viscous diffusion is much less than the oscillation ( $\omega^{-1}$ ), i.e.  $\rho_f \omega w^2 / \mu \ll 1$ , or for time-independent problems, the time derivative term in Eq. (4) can be neglected, time-dependent flow fields can be regarded as quasi-steady Stokes flows described by Eqs. (2) and (5):

$$0 = -\nabla p + \mu \nabla^2 \mathbf{u} + \mathbf{F}. \quad (5)$$

In a simple flow system and channel geometry, Eq. (5) can be further solved through various analytical approaches (Anderson and Idol 1985; Ajdari 1995; Qian and Bau 2002; Thamida and Chang 2002; Yossifon et al. 2006).

Recently, the lattice Boltzmann (LB) equation has been proven useful for the description of mesosystems with complicated geometry and composition (Succi 2001). Hence, it also has been widely used over the past years to describe the electrokinetic flow field and mixing (Tian et al. 2005; Wang et al. 2005a, 2006a; Tang et al. 2006), which is solved through the so-called lattice Boltzmann method (LBM).

## 2.1 Visualization of micro-mixing

The majority of the numerical studies of micromixing solved the convection-diffusion equation, Eq. (6), to visu-

alize the mixing process and evaluate the mixing performance:

$$\frac{\partial C}{\partial t} + \mathbf{u} \cdot \nabla C = D \nabla^2 C, \quad (6)$$

where  $C$  and  $D$  represent the sample concentration and diffusivity, respectively. Note that the electrophoretic effect is not considered in the convective term of Eq. (6), but it should be considered when the samples are not neutral dyes or biological elements. However, there are several drawbacks to this approach. For example, if the deformation of the interface is complex and the mixing channel is too long, solving this equation may fail to identify the precise interface due to numerical diffusion and species diffusion in nature. Furthermore, for large Péclet number cases, convective transport dominates diffusive transport; in this case, dispersion of the sample in the flow field can be greatly enhanced by promoting the convective transport. In such diffusion-limited cases, the diffusion effects can be neglected; the sample just convects with the fluid along the local instantaneous streamlines. Then, the Lagrangian particle tracing technique which places mass-less, non-interacting passive particles in the flow fields to observe the advection of tracer particles is sufficient to provide the information on the sample mixing process in the unsteady flow field without solving Eq. (6). The motion of a tracer particle can be tracked by the kinematic equation (dynamic system):

$$\frac{d\mathbf{r}}{dt} = \mathbf{u}(\mathbf{r}, t), \quad (7)$$

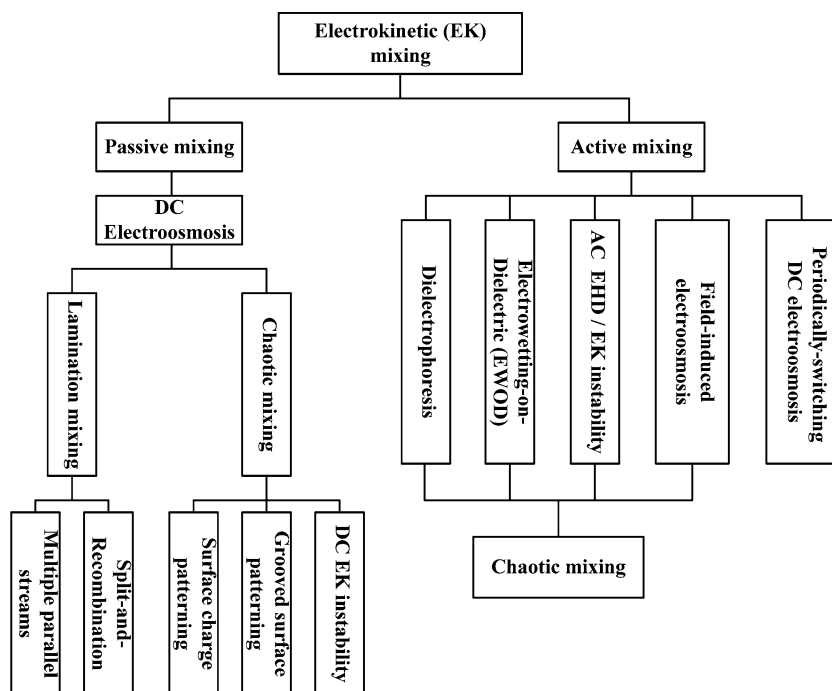
where  $\mathbf{r}$  is the location of the tracer particle and  $\mathbf{u}(\mathbf{r}, t)$  is the Eulerian velocity field. The tracer particle position in the time-independent or dependent flow field at different times can be obtained by integrating Eq. (7). Many integration methods are presented in the literature, ranging from the simple first-order Euler method to the fourth-order Runge-Kutta method or even higher-order methods (Spratt 2003). Besides, when using the particle tracing method to simulate the dispersion of a blob of samples, the stretching and folding of fluid elements effects in a time-dependent flow field can be clearly observed.

In experiments from the literature, the velocity fields in micromixers were usually measured through micro-particle image velocimetry (micro-PIV), while mixing patterns were visualized through fluorescence or confocal fluorescence microscopy. Confocal fluorescence microscopy was usually used to observe the three-dimensional structure of steady flow mixing. Regarding microflow visualization, interested readers can refer to the excellent review paper by Sinton (2004) for more details.

## 2.2 Characterization of chaotic mixing

In order to understand and optimize fluid deformation in micromixers during the mixing process, it is necessary to understand the mechanism of fluid stretching and folding, and evaluate them in a quantitative manner. In the past two decades, it has been demonstrated that chaotic mixing is associated with such stretching and folding of fluid elements described by dynamic system techniques such as Poincaré maps and Lyapunov exponents. Regarding the information of Poincaré maps and Lyapunov exponents, interested readers can refer to the references for more details, e.g. Ottino (1989), Wolf et al. (1985) and Sprott (2003). The velocity field of micromixers used to describe Poincaré maps and Lyapunov exponents is obtained through either theoretical analysis or micro-PIV measurements (Suzuki et al. 2004). Using the combination of Poincaré maps and Lyapunov exponent analysis, the chaotic characteristics of micro-mixing systems can be described thoroughly. Poincaré maps can be used to explain the process of the mixing system from periodic or quasi-periodic to chaos, while the Lyapunov exponent can be used to measure the strength of the chaotic behaviors and then provide information of the effects of parameters such as the surface topology, amplitude and frequency of perturbation to chaos; it can also be used to optimize the design and operation of mixing micro-devices. A positive Lyapunov exponent means chaotic behavior. Larger Lyapunov exponents indicate that the system is more chaotic.

**Fig. 3** Classification scheme for microfluidic mixing based on electrokinetics



## 3 Micro-mixing based on electrokinetics

In this review, electrokinetic mixing is categorized as either active or passive mixing, as shown in Fig. 3. Passive mixing refers to the mixing effect in electrokinetically driven systems and is enhanced by virtue of their particular geometry topologies, surface properties, or instability phenomenon which occurs naturally under a static (DC) electric field. Active mixing refers to the enhancement of mixing in electrokinetically driven microfluidic systems using a time-dependent electric field or in pressure-driven flow systems by means of an externally time-dependent or independent electrical force. Chaotic mixing can be achieved by means of the following schemes: dielectrophoretic (DEP) force perturbation, the shaking of electrowetting-based droplet, DC/AC EKI (or EHD) instability, field-induced electroosmosis, and surface charges or grooved surface patterning.

### 3.1 Passive mixing

In general, electrokinetic passive mixing can be categorized as either lamination or chaotic mixing. In the case of lamination mixing, mixing mainly relies on the molecular diffusion effect between two or more parallel streams, while chaotic mixing usually refers to the interfacial contact area between two mixing streams. In chaotic mixing, this area is greatly increased and the diffusion length is reduced by means of the repeated stretching and folding of the fluids in a microchannel.

3.1.1 *Mixing of multiple parallel electroosmotic streams based on molecular diffusion*

T- or Y-shaped microchannels with two inlets were common microfluidic devices for the mixing of analytes and reagents in the literature (Kamholz et al. 1999; Ismagilov et al. 2000). Two streams of distinct species are injected side-by-side into a single microchannel. Mixing of the streams is only through molecular diffusion across their common interface. Furthermore, Jacobson et al. (1999) proposed an electroosmotic-based microfluidic device designed with series T-intersections capable of multiple samples parallel mixing, as shown in Fig. 4a. The device was tested by mixing a sample with buffer in a dilution experiment. Figure 4b shows that mixing images and signal responses for seven individual analysis channels generates calculated sample fractions of 1.0, 0.84, 0.67, 0.51, 0.36, 0.19, and 0 in this parallel mixing device.

In the literature, the major portion of the microfluidic mixing studies is two species mixing within one inlet stream in a microchannel. Hence, parallel lamination mixing generally refers to the inlet mixing stream being split into two or more sub-streams, and then joins them horizontally as individual laminae in a single stream. Particularly, the concept of reducing diffusion length for parallel lamination mixing is known as hydrodynamic focusing (Knight et al. 1998). In this technique, the microfluidic device is designed with three inlets, as shown in Fig. 5a. The sample (solute) flow is introduced through the middle inlet, while the solvent streams are fed through the side inlets; these function as sheath flows to restrict the

width of the sample flow and consequently reduce the diffusion length. Similarly, the flow focusing effect can also be controlled using electroosmotically driven flow, which is called electrokinetic focusing (Jacobson et al. 1997; Yang et al. 2006), as shown in Fig. 5b. Knight et al. (1998) reported that the sample stream width ( $w_f$ ) can be focused to 50 nm, resulting in a mixing time of no more than a few microseconds ( $t_m \sim w_f^2/D$ ). This rapid diffusion-based mixer has been successfully integrated with microfluidic platforms to enable the accurate description of fast chemical reaction kinetics such as protein folding (Pollack et al. 1999; Hertzog et al. 2004). The rapid mixing based on the hydrodynamic focusing approach was also extended to multiple stream mixing in pressure-driven flow system, namely “SuperFocus” micromixing (Hessel et al. 2003; Hardt and Schönfeld 2003; Löb et al. 2004). Figure 6a shows an example of the SuperFocus micromixing with 138 interdigital streams. The streams were injected separately from many inlets and then joined as individual laminae in a single stream in the downstream channel. Thus, lamination parallel mixing is greatly improved due to diffusion length (striation thickness) reduction. Similarly, Wang et al. (2005b) and Wu and Yang (2006) also used multi-stream electrokinetic focusing to improve lamination mixing, as shown in Fig. 6b. Although it can be used to enhance micromixing, there is one problem to be considered and resolved regarding the integration of microfluidic system: how to split two mixing streams from two inlets into multiple parallel streams. In prior studies (Löb et al. 2004; Wu and Yang 2006), these streams (six streams) were injected separately from multiple inlets (six inlets);

**Fig. 4** **a** Schematic of the microfluidic chip for electroosmotic parallel mixing. “S”, “B”, “A”, and “T” refer to the sample, buffer, analysis channel, and intersections, respectively. The channels are represented by double lines. **b** Fluorescence image and signal for parallel mixing of the sample with buffer (Jacobson et al. 1999)

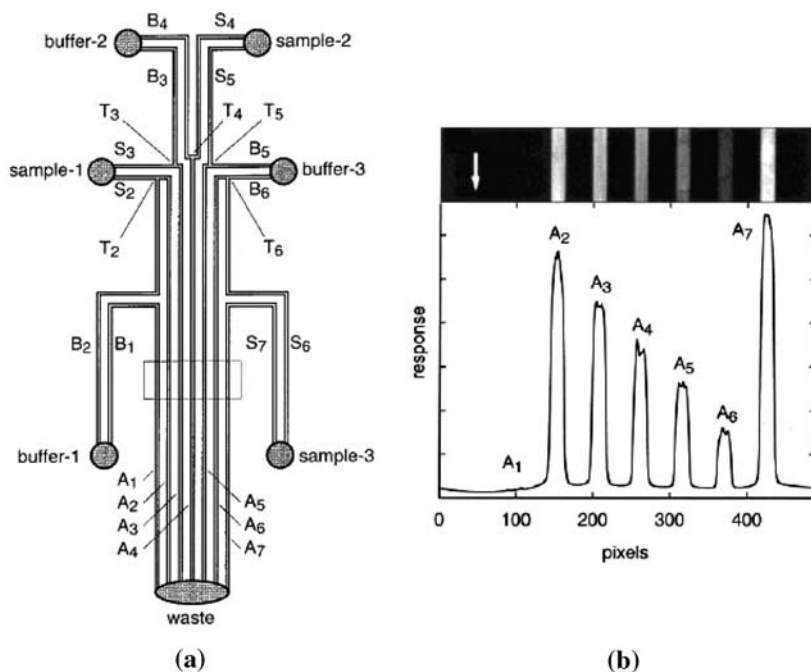


**Fig. 5** Fluorescence images of rapid mixing in **a** a hydrodynamic focusing device (Knight et al. 1998) and **b** an electrokinetic focusing device (Jacobson et al. 1997). The width focused sample stream ( $w_f$ ) is smaller and indicates that the mixing is faster

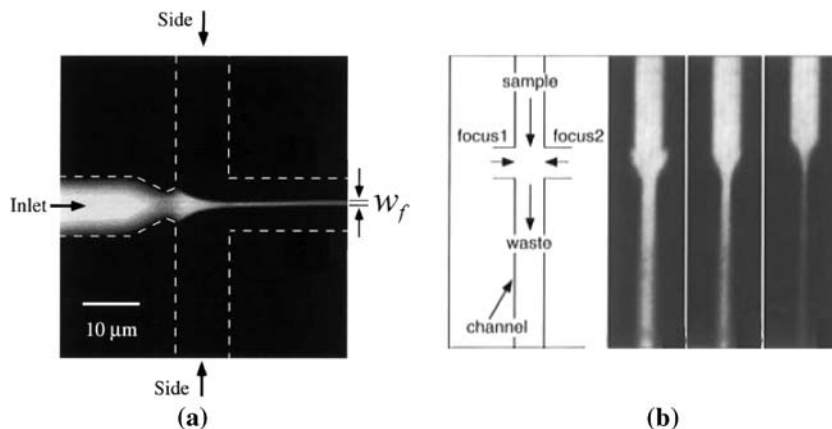


**Fig. 6** **a** Multi-stream mixing with hydrodynamic focusing (Löb et al. 2004) and **b** with electrokinetic focusing (Wu and Yang 2006)

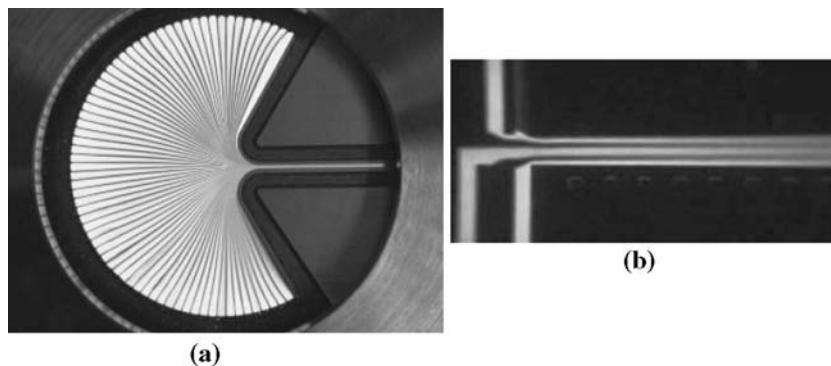
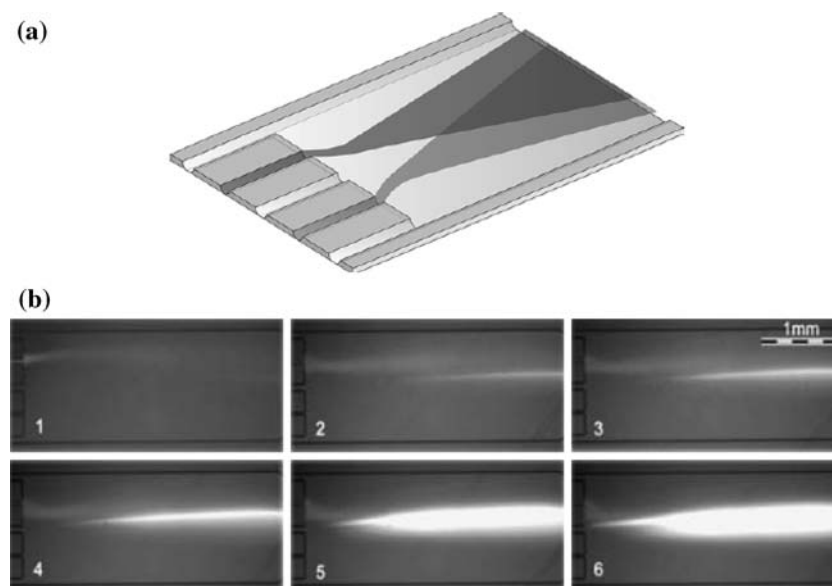


**Fig. 7** **a** Schematic illustration of the two sample electroosmotically address-flow device used as a microreactor. **b** Fluorescence images of the intensity of the reaction product fluo-4/ $\text{Ca}^{2+}$  for different distances between two reactant streams (Kohlheyer et al. 2005)



this is not practical in microfluidic systems. This problem is not easily solved in in-plane microchannel structures, but it may be solved by the design of out-of-plane microchannel structures. In addition, Kohlheyer et al. (2005) proposed an adjusted multi-stream diffusion-based microreactor using electroosmotic guiding flow streams composed of two sample inlets, three guiding buffer inlets, and one reaction chamber, as shown in Fig. 7a. The region

where the molecular diffusive profiles of two parallel sample streams overlap is used for the reactions. The size of the region (or the distance between two sample streams) can be adjusted by changing the flow rate ratio of three guiding buffer streams. Figure 7b shows the reactions of two reactant streams (one consists of buffer and fluo-4, and the other consists of buffer and  $\text{CaCl}_2$  solution) at different distances between two parallel reactant streams. In prin-



ciple, this parallel lamination mixing device can also be categorized as an active mixer or reactor since the mixing is controllable.

### 3.1.2 Split-and-recombine (SAR) lamination mixing

In contrast to the multi-stream lamination mixing mentioned above, the SAR lamination mixing relies on a multi-step procedure, as shown in Fig. 8a. Three basic steps are required: fluid element splitting, recombination, and rearrangement. The three steps can be completed when the two mixing streams flow through an out-of-plane microchannel structure, as shown in Fig. 8b (Schönfeld et al. 2004). After one SAR step, the two streams can be split into four lamellae. Then, the interfacial contact area is increased by double and the diffusion length is reduced to a half of channel width ( $w$ ). The lamellae dimension depends on the number of SAR steps ( $n$ ). The diffusion length after  $n$  SAR steps leads to an exponential decrease of  $w/2^n$ , and exhibits an exponential increase of the interfacial contact area. Thus, a positive Lyapunov exponent can be achieved by means of a SAR mixing scheme at a low Reynolds regime (Schönfeld et al. 2004; Hardt et al. 2006); then this approach was also termed as “uniform chaotic mixing” in their studies. Although this mixing scheme was only successfully applied to the pressure-driven flow mixing in the previous studies and no other literature regarding split-and-recombine electroosmotic flow mixing has been noted, it may be suitable for the electroosmotic flow system. Since the mixing scheme requires a series of out-of-plane

microchannel structures for splitting and recombining flows, it may not be easily integrated into microfluidic systems.

### 3.1.3 Grooved surface enhanced electroosmotic mixing

Stroock et al. (2002a) proposed a chaotic mixing channel with patterned grooves for pressure-driven flow system. The transverse flows can be produced in the grooved channels which result in a helical flow motions at a low Reynolds number regime (Stroock et al. 2002a, b; Stroock et al. 2003). Similarly, helical flow motion also can be achieved for electroosmotic flow in grooved microchannels (Johnson et al. 2002), as shown in Fig. 9. Since the slanted groove design of this mixing channel is able to induce a lateral transport across the channel (see Fig. 9c), the mixing is not limited by molecular diffusion. From Fig. 9a, it is seen that the incoming fluorescent stream was split into two streams after four slanted grooves at a flow velocity 0.81 cm/s, corresponding to a Reynolds number 0.45. Although the mixing is improved after the slanted grooved region, the stream splitting phenomena still results in poor mixing due to the lack of repeated stretching and folding of the fluid in the downstream channel. To avoid splitting the stream and to achieve complete mixing, another design shown in Fig. 9b was also proposed. In addition, it also can be avoided by means of periodic staggered herringbone grooves, as proposed by Stroock et al. (2002a). Once the induced transverse flow is strong enough for efficient lateral transport, it will conform to the LTM idea (Ottino and Wiggins 2004b; Wiggins and Ottino 2004); then, electroosmotic flow chaotic mixing can be induced. Johnson and Locascio (2002) also investigated the numerical effect of the groove angle relative to the channel axis, the groove depth, and the zeta potential (i.e. surface charge density) ratio of groove to main channel on electroosmotic flow mixing over periodic slanted grooves. The numerical results show that mixing performance was improved by increasing the groove depth, decreasing the groove angle, and increasing the magnitude of the zeta potential ratio. The effect of surface charge patterning on electroosmotic flow mixing will be discussed in the following section.

### 3.1.4 Heterogeneous surface charge patterning enhanced electroosmotic mixing

According to the theory of similitude between electroosmotic flow velocity and electric field (Cummings et al. 2000), the electroosmotic flows streamlined in uniform zeta potential microchannels are the same as the electric field lines governed by the electric vector field ( $\mathbf{E}$ ). As a result, the flow velocity and electric vector fields are both irrotational. Electroosmotic flow fields are unique in that they

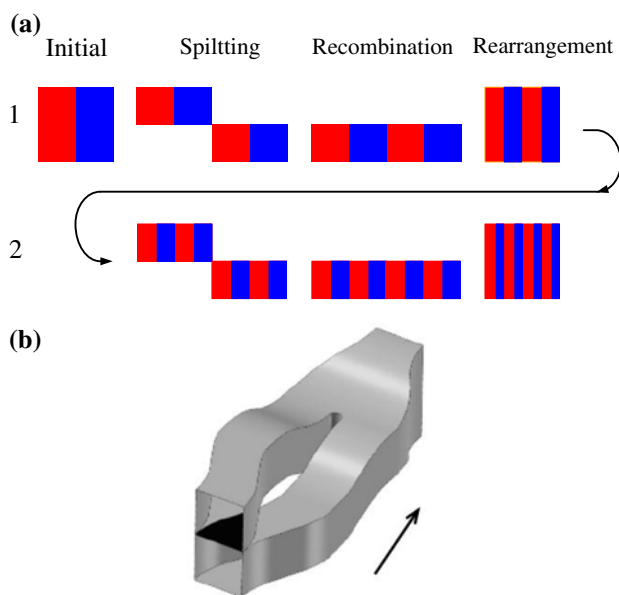
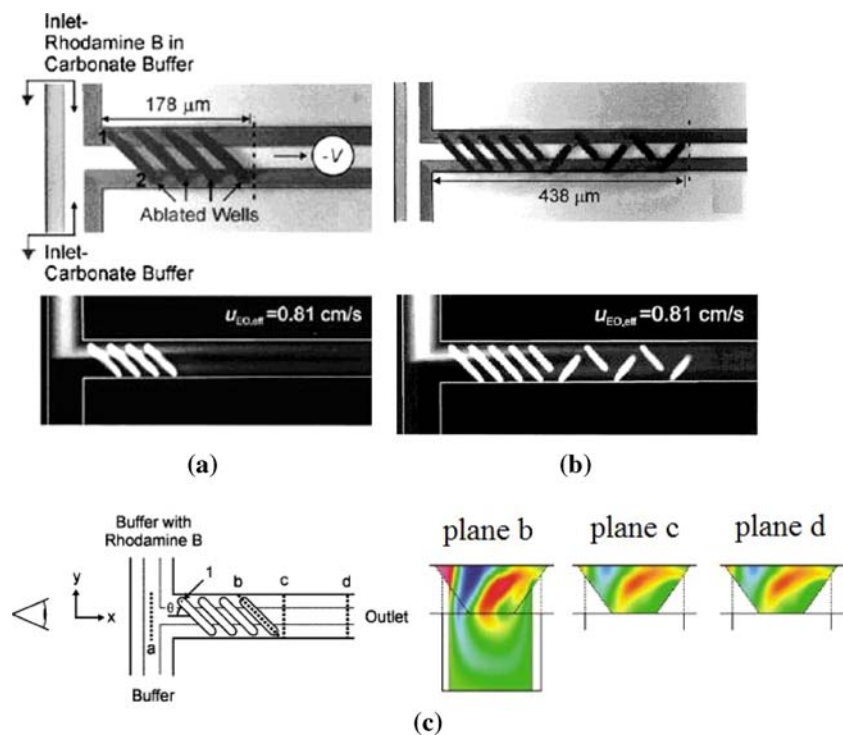


**Fig. 8** **a** Schematic illustration of split-and-recombine mixing scheme. **b** One split-and-recombine unit (Schönfeld et al. 2004). The arrow indicates the flow direction

**Fig. 9** The pattern configurations of two different slanted grooves (wells) and fluorescence images of mixing in a T-shaped microchannel (**a** and **b**) at a Péclet number of  $Pe = 1500$  (Johnson et al. 2002). **c** Simulation results of species mixing in configuration (**a**) for a groove angle of  $\theta = 15^\circ$  and a groove depth of  $50 \mu\text{m}$  at a Péclet number of  $Pe = 700$  (Johnson and Locascio 2002)



can also be described as a potential flow due to the slip condition. However, the irrotational feature of potential flow implies that closed streamlines and vortices are impossible to be generated. Surfaces with non-uniform zeta potentials are one way to produce vortices or specific flow structures in electroosmotic flow fields. Hence, the surface properties of the microchannel play an important role in controlling surface-driven electroosmotic flow (Stroock and Whitesides 2003) and can be exploited to produce specific flow structures to improve the mixing performance. Anderson and Idol (1985) and Ajdari (1995) performed a theoretical investigation into electroosmotic flows induced by a non-uniformly distributed zeta potential along the pores and microchannel walls, and suggested that the application of oppositely charged surface heterogeneities to the microchannel walls generated recirculation regions within the bulk flow near the heterogeneous regions. This flow phenomenon was observed experimentally by Stroock et al. (2000). In later studies, these induced localized circulations in the steady flow field were successfully employed to improve species mixing in a microchannel (Erickson and Li 2002; Chang and Yang 2004; Fushinobu and Nakata 2005; Wang et al. 2005a; Tang et al. 2006) or a curved microchannel (Lin et al. 2006). However, chaotic mixing was absent in the proposed mixers since the zeta potential was time-independent and hence the induced circulations were closed and steady in two-dimensional flow systems. To achieve chaotic advection in two-dimensional flow systems, these circulations must be

broken in some way. For example, various researchers have performed theoretical studies of electroosmotic flows in 2-D microchannels driven by time-dependent zeta potentials or a time-dependent external electric field, and have demonstrated that chaotic advection can be induced by time-wise periodic alternations of the zeta potential and can improve the mixing performance as a result (Qian and Bau 2002); these are to be described in the section of active mixing scheme. In addition, chaotic advection or transverse flows can also be induced in three-dimensional steady electroosmotic flows with time-independent zeta potentials through the use of specific surface charge patterning configurations (Ajdari 1996, 2001; Erickson and Li 2003; Ng et al. 2004; Yang and Chang 2004; Biddiss et al. 2004; Chang and Yang 2006). Generally, heterogeneous surface charges or non-uniform time-independent zeta potentials are obtained through passive approaches such as coating the microchannel walls with different materials (Liu et al. 2000; Stroock et al. 2000; Fushinobu and Nakata 2005) or applying suitable surface-chemistry treatments (Hau et al. 2003; Krishnamoorthy et al. 2006).

Biddiss et al. (2004) used a polybrene-coated method proposed by Liu et al. (2000) to create a non-uniform zeta potential distribution on the bottom of a PDMS microchannel, as shown in Fig. 10a. The electroosmotic mobilities of native-oxidized PDMS and polybrene-coated surfaces for sodium carbonate/bicarbonate buffers of pH 9.0 were measured to be  $-5.9 \times 10^{-8}$  and  $2.3 \times 10^{-8} \text{ m}^2/\text{V s}$ , which correspond to the zeta potentials of  $-83$  and  $32 \text{ mV}$ ,

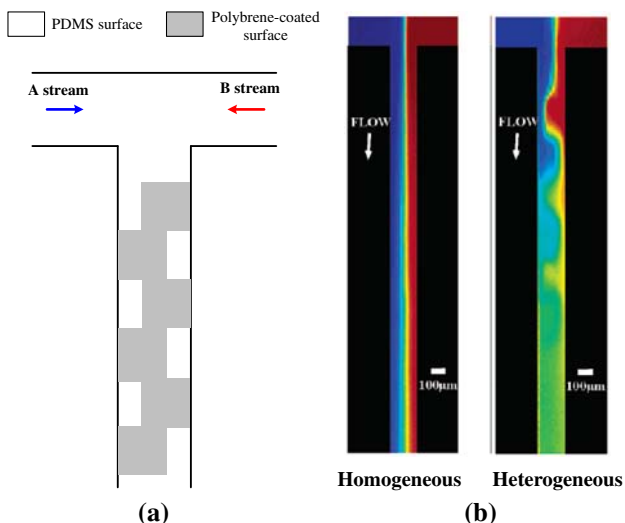
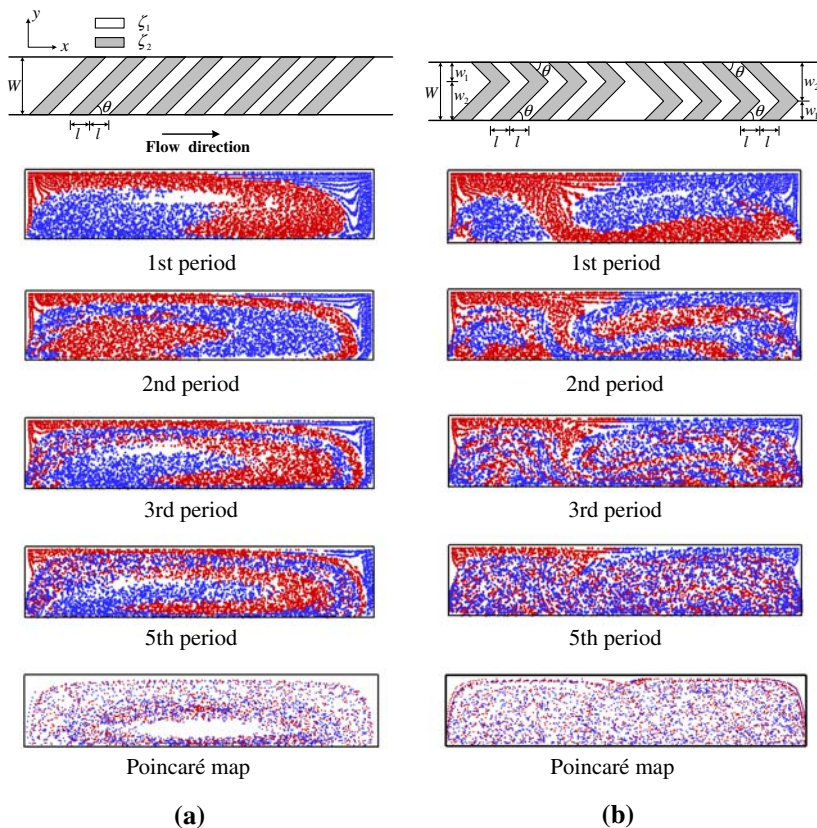


**Fig. 10** **a** Heterogeneous surface charge patterning configuration in a T-shape microchannel. **b** Experimental image of species mixing in the homogeneous and heterogeneous charged microchannel (**a**) for an electric field strength of 280 V/cm corresponding to a Péclet number of  $Pe = 760$  (Biddiss et al. 2004)

respectively. The ratio of the zeta potential of the heterogeneous surface to that of the channel wall is  $-0.38$ . In this mixing channel, the channel wall with negative zeta potential drives the flow along the net flow direction, while the heterogeneous surface with a positive zeta potential

tends to stop the flow. To satisfy continuity, transverse flow components must be induced in the heterogeneous regions (i.e. transverse pressure gradients are induced), resulting in secondary flows within the mixing channel. In Fig. 10b, it can be seen that the transverse flow was induced and the mixing was greatly enhanced in the heterogeneous microchannel; also, the channel length required for complete mixing is reduced to 2.6 mm, which is much shorter than the value 22 mm for mixing in a homogeneous microchannel. In addition, Chang and Yang (2006) also employed a particle tracking method to visualize the fluid mixing process from a cross-section perspective in heterogeneous microchannels, as shown in Fig. 11. The mixing channels considered in their study were characterized by a periodically repeating mixing protocol. To clearly observe the dynamics of the mixing process, the positions of each particle were recorded at the outlet of the computational domain of each period. Figure 11a shows that clockwise transversely rotational flows with an elliptic region (i.e. an unmixed island) are generated in the microchannel. The elliptic region, similar to a “cat’s eye” structure, is also clearly visible in the Poincaré maps shown in Fig. 11a. According to Kolmogorov–Arnold–Moser (KAM) theorem in the dynamic system (Ottino 1989; Sprott 2003), the fluid in this region cannot mix with their surroundings (without a molecular diffusion effect). Thus, the mixing is locally chaotic in the mixing channel with patterned straight

**Fig. 11** Visualization of mixing at different periods in microchannels with **a** straight diagonal heterogeneous strips and **b** staggered asymmetric herringbone heterogeneous strips; its Poincaré maps are obtained from particle tracing for 200 periods with 20 particles. The zeta potential ratio of the heterogeneous strip ( $\zeta_2$ ) to channel wall ( $\zeta_1$ ) is  $-0.5$  (Chang and Yang 2006)



diagonal heterogeneous strips. In contrast, the unmixed island vanishes in Fig. 11b and the global chaotic mixing is induced. The concept of this design is similar to that of the staggered herringbone mixer (SHM) proposed by Stroock et al. (2002a) and also fits within the LTM framework (Ottino and Wiggins 2004b; Wiggins and Ottino 2004). It is seen that two unequal counter-rotating vortex flows (i.e. a blinking vortex) exist in this mixing system. The blinking vortex provides the main transport mechanism of the two different colored particles from left to right and right to left in a periodic manner. From Fig. 11a and b, it should also be noted that in addition to the particles near the bottom wall, the particles near the channel walls are not easily stirred. This is because the electroosmotic flow is surface-driven and hence the streamwise velocity near the walls is larger than the transverse flow velocity. Hence, the results show that the mixing efficiency decreases as the channel aspect ratio (channel height-to-width) increases in their study. This may be a reason why the channel is designed to be a low aspect ratio (approximately 0.04) in the study of Biddiss et al. (2004). The mixing in heterogeneous microchannels with a higher aspect ratio may be improved by increasing the magnitude of the zeta potential ratio. This is because a higher magnitude of the zeta potential ratio generates a stronger secondary flow (Chang and Yang 2006).

One important effect on the electroosmotic flow transport is not mentioned above and should be considered for the mixing in heterogeneous microchannel. Because the continuity condition must be satisfied, the axial pressure gradients, except the transverse pressure gradients, are also induced in a non-uniform zeta potential microchannel (Herr et al. 2000; Ren and Li 2001; Fu et al. 2003), which may result in a reduced net flow rate of electroosmotic flow in microchannels, especially for the high magnitude of the zeta potential ratio. Therefore, the tradeoff between electroosmotic flow mixing and transport should be considered in this mixing scheme (Tian et al. 2005).

### 3.1.5 DC electrokinetic instability (EKI) mixing

The electrokinetic instability (EKI) phenomenon was first observed experimentally in microfluidics by Oddy et al. (2001). This instability phenomenon is not due to mechanisms such as time-modulated electric fields (Suresh and Homsy 2004) and Joule heating effects (Chang and Homsy 2005). It is described by charge accumulation at perturbed interfaces due to electrical conductivity gradients,  $\nabla\sigma$ , which exist in the bulk flow (Lin et al. 2004b; Chen et al. 2005). The net charge density in the bulk liquid derived from electrostatics theory can be expressed as

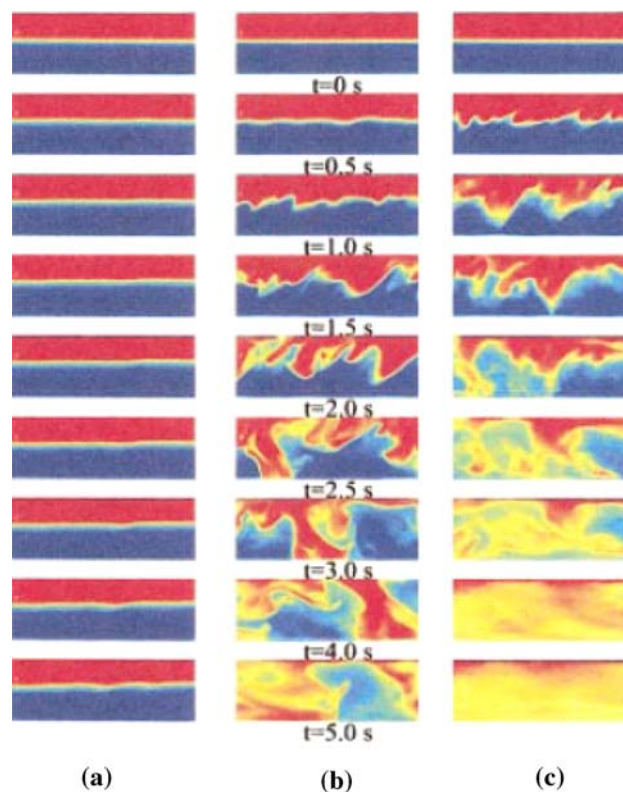


**Fig. 12** Experimental images of electrokinetic instability phenomenon under different DC electric field strengths of **a** 250 V/cm, **b** 500 V/cm, and **c** 750 V/cm (Lin et al. 2004b)

$$\rho_e = -\frac{\varepsilon \mathbf{E} \cdot \nabla \sigma}{\sigma}, \quad (8)$$

where  $\varepsilon$  is the permittivity of the electrolyte and  $\mathbf{E}$  is the external electric field. Then, it results in an electrical force ( $\rho_e \mathbf{E}$ ) which distorts the interface, as shown in Fig. 12. This mechanism is similar to that of electrohydrodynamic instability as proposed by Hoburg and Melcher (1976, 1977). The differences between them are that the electroosmotic effect and molecular diffusion effect of electrical conductivity are considered in EKI model (Lin et al. 2004b; Chen et al. 2005; Posner and Santiago 2006). The onset of instability is governed by an electrical Rayleigh number, which represents the relative importance of electrical body forces to dissipative forces due to molecular and viscous diffusion.

$$Ra_e = \frac{U_{ev} h}{D_{eff}}, \quad (9)$$

describes the case where  $U_{ev}$  is electro-viscous velocity generated from the electrical force balanced by the viscous force,  $h$  is length scale of channel width and  $D_{eff}$  is effective diffusivity of electrolyte. The electrical force plays a role in destabilization of the electrokinetic flow,

while the flow is stabilized by the dissipative forces. Thus, the flow field is conditionally unstable. The critical electrical Rayleigh number has been found to be approximately 10 in the case of an electric field perpendicular to the electrical conductivity gradients in thin microchannels through a linear stability analysis (Chen et al. 2005). Over this critical value, the unstable flow can be generated. In addition, the ratio of electro-viscous to electroosmotic velocities (i.e. Smoluchowski velocity) governs the onset of absolute instability; the critical value of this ratio is approximately 4 (Chen et al. 2005). The absolute instability always occurs at a high intensity of the electric field.

Recently, this instability flow has also direct applications to rapid electrokinetic passive mixing in a DC field (Park et al. 2005; Tai et al. 2006; Huang et al. 2006). However, there are two disadvantages of the application of electrokinetic instability flow to microfluidic mixing. One is that the electrical conductivity gradients must exist in the bulk flow (i.e. two flow streams with different conductivities are required); the other is that a high electric field strength is required. In general, the critical strength of the electric field resulting in unstable flow decreases as the conductivity ratio is increased, but still there is a limitation (Chen et al. 2005; Posner and Santiago 2006). For a fixed electric field, the experimental results also show that the mixing performance is greatly enhanced in the case of high conductivity ratios when compared to the case of low conductivity ratios (Huang et al. 2006). Unfortunately, the conductivities of various sample and buffer streams in microfluidic systems are either unknown or poorly controlled. In Fig. 12, it can be seen that a more chaotic flow induced by a higher intensity of electric field ( $>500$  V/cm) to achieve efficient mixing when an electrical conductivity ratio is 10, while the value of the electric field strength is in general too large for practical microfluidic systems. The electrokinetic convective instability flows usually occur at a relatively lower electric field strength compared to that of absolute instability flows (Chen et al. 2005). However, the convective instability flow in microchannels always shows a periodic motion in the downstream and results in poor chaotic mixing. More chaotic mixing may be achieved under a lower electric field by breaking the periodic behavior in some ways, e.g. use of the specific designs of channel geometry (Park et al. 2005; Tai et al. 2006; Huang et al. 2006) or patterned porous structures (i.e. block) in the mixing channel. As shown in Fig. 13, the peak of the unstable wave is pulled to the corner by strong electrical forces (note: net charge density calculated from Eq.(8) has a negative value at the corners) due to there being a high electric field at the cavity corners when the unstable wave approaches to the cavity corners (Park et al. 2005). The wave remains attached to these corners (i.e. stagnation points), and the interface is stretched repeatedly along the

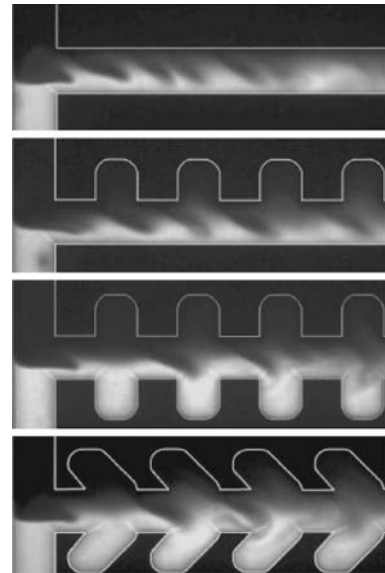


**Fig. 13** Experimental images of electrokinetic instability phenomenon for different channel geometries at an electric field strength is approximately 300 V/cm. Here conductivity ratio is 10 (Park et al. 2005)

downstream resulting in a more unstable or chaotic flow pattern. In addition, more chaotic flow patterns can also be achieved by applying time-periodic electric fields (Shin et al. 2005); this is described in the section of AC electrokinetic instability mixing.

### 3.2 Active mixing

In general, the choice of driving amplitudes and frequencies, and optimization of operation conditions is a challenge in designing an active micro-mixer. Under appropriate operation conditions, the major portion of electrokinetic active mixing schemes in the literature is able to induce chaotic mixing, except the case of periodically switching electroosmosis mixing enhancement.

#### 3.2.1 Dielectrophoretic-based mixing

Dielectrophoresis (DEP) refers to the polarization of a particle or biological element relative to a suspension medium in a non-uniform electric field which results in motion (Morgan and Green 2003; Jones 2005). Positive DEP forces moves particles to regions with a higher electric field (i.e. near the electrode edges), while the particles are repelled from the electrode edges to a lower electric field by negative DEP forces. The positive or negative DEP force is only induced by applying the specific range of the frequency of the AC field, which is dependent on the permittivity of the biological element and suspension medium (i.e. Clausius–Mossotti factor). Lee et al. (2001) and Deval

et al. (2002) have used dielectrophoretic forces as a perturbation source to facilitate chaotic mixing in simple microchannel geometry. It takes advantages from the relatively high magnitude of the DEP force compared to other forces acting on micron or submicron biological elements. The main stream in their device is driven by a syringe pump. The working unit is composed of cavity and electrodes, as shown in Fig. 14. The saddle point regions can be generated when the positive or negative DEP force is large enough to overcome hydrodynamic force, where particle distributions are stretched and folded, resulting in chaotic trajectories as shown in Fig. 14 (note: saddle point refers to the mathematical definition of bifurcation in a dynamic system (Sprott 2002)). The chaotic strength of this mixing system depends on the cavity geometry, electrode distribution, and the combination of fluid velocity, electric field strength and electric field actuation frequency (i.e. frequency switches between positive and negative DEP forces). In addition, the particle distribution would be more homogeneous across the channel width downstream after more and more working units. This is because the particle distribution is stretched and folded repeatedly.

### 3.2.2 Electrowetting-on-dielectric (EWOD) droplet-based mixing

Electrowetting refers to that the wetting properties of a droplet in contact with an insulated electrode which can be altered by means of an electric field. If an electric field is applied non-uniformly on an electrode array, a surface energy gradient is induced which can be used to manipulate the motion of the droplet (Lee et al. 2002; Moon et al. 2002). Multiple-electrode arrays allow for manipulation of a large number of droplets independently. Recently, an electrowetting-based digital microfluidic system was

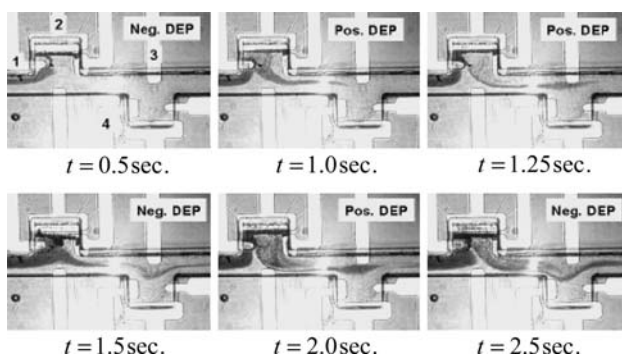


**Fig. 14** Stretching and folding of particle distribution in a time-series. Average flow velocity of the main stream is maintained at 500  $\mu\text{m/s}$  and  $\pm 10$  V. AC voltage is applied between electrodes 1 and 2 and between 3 and 4. AC frequency switches between 700 kHz (positive DEP) and 15 MHz (negative DEP) at a rate of 0.5 s (Deval et al. 2002)

developed and provides a path toward realizing the true lab-on-a-chip in the future (Fair 2007). The analytes and reagents are transported in this system through the motion of discrete droplets rather than continuous flow streams. The droplets act as a virtual mixing chamber, and an active mixing scheme was developed by shaking the merged droplet (Paik et al. 2003a). Complex flow patterns inside the merged droplet can be induced to greatly enhance mixing during droplet oscillating motion on one dimensional four-electrode arrays at an appropriate switching frequency. The results show that the fastest time for mixing two 1.3  $\mu\text{l}$  droplets was about 4.6 s in a linear oscillation on four electrodes at a frequency of 16 Hz. An alternative rapid droplet mixing scheme, split-and-merge droplet mixing on one-dimensional three-electrode array, was also proposed by Paik et al. (2003b), as shown in Fig. 15. It can be seen that splitting and remerging resulted in a rapid mixing of two 0.8  $\mu\text{l}$  droplets within 1.7 s.

### 3.2.3 Electrohydrodynamic (EHD) instability mixing

Electrokinetic force generally refers to the force generated by the interaction between electric field and net charge density near the solid–liquid interfaces. Electrohydrodynamics (EHD) also includes forces that act away from solid–liquid interfaces in regions where the bulk liquid has conductivity and permittivity gradients in addition to the electrokinetic force. Over past years, EHD studies typically deal with near-dielectric liquids (e.g. oil, alcohol,

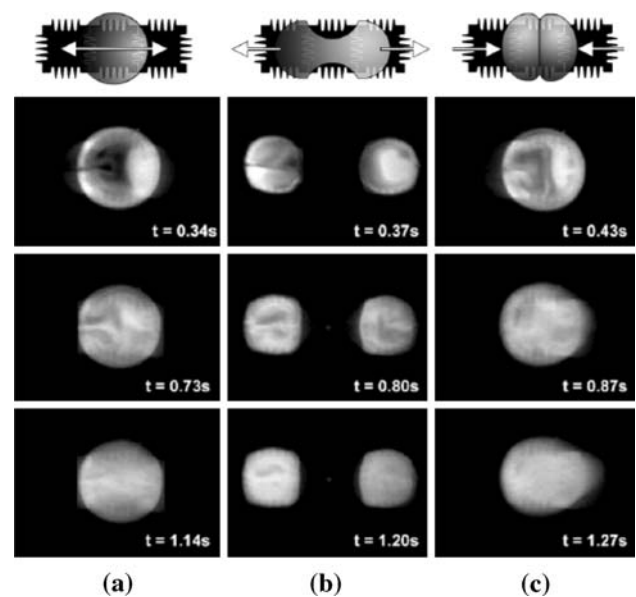


**Fig. 15** Experimental images of a droplet mixing on a three-electrode array with splitting and merging. **a** A merged droplet is oscillated across the three electrodes at a frequency 16 Hz. **b** The droplet is then split into two droplets and then remerged (**c**) at the same frequency (Paik et al. 2003b)

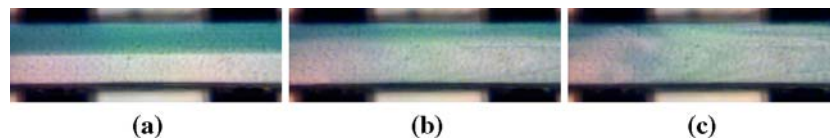


**Fig. 16** Experimental images of electrohydrodynamic mixing under a DC electric field. **a** Initial condition, **b** intensity of electric field is 4 kV/cm, and **c** 6 kV/cm (El Moctar et al. 2003)

etc.) and can be described by the Taylor–Melcher leaky-dielectric model (Saville 1997). The electrokinetic effect in EHD studies usually can be neglected due to the liquid being non-conducting to form polarized layer at solid–liquid interface (i.e. electrical double layer). As mentioned in EKI mixing, the EHD instability phenomenon may also be induced due to electrical conductivity gradients existing in the bulk liquid (Hoburg and Melcher 1976, 1977). Hoburg and Melcher (1976, 1977) performed an experimental and stability analysis for an electric field parallel or perpendicular to the liquid–liquid interface (corn oils with different conductivities). Recently, a microfluidic mixer was developed by El Moctar et al. (2003) utilizing an electrohydrodynamic instability phenomenon. In the micromixer, two fluids with identical viscosity and density (oil) but different electrical properties (e.g. conductivity and permittivity) were injected into the mixing channel by syringe pumps; the electrodes were arranged in such a way that the electrical field was perpendicular to the species interface, as shown in Fig. 16, creating a chaotic flow. The average flow velocity of main stream was 4 mm/s, corresponding to a low Reynolds number of approximately 0.02. The mixing effects induced by both DC and AC electric fields were explored in a series of experimental investigations. In Fig. 16, it can be seen that the mixing becomes more chaotic as the intensity of the DC electric field increases. In the case of AC fields, the mixing is only greatly enhanced under the lower frequency electric field. This is because the free charges do not have enough time to build up in the bulk flow when the period of AC field is much smaller than the charge relaxation time scale (approximately 0.68 s for corn oils). The results revealed that the application of an appropriate voltage and frequency to the electrodes yielded a satisfactory mixing performance within less than 0.1 s over a short mixing distance, even at Reynolds numbers as low as 0.02. In their experiments, the electrochemical (Faradic) reaction on the electrodes was not observed and no bubbles were generated in mixing channel under a DC field or a low frequency AC field due to the working fluid is corn oils. In general, DC voltages in excess of 2 V will produce bubbles when electrodes in contact with typical electrolyte solutions. Consequently, the design of this EHD mixer is not suitable when the fluids are aqueous solutions. To avoid bubble generation

inside microchannels when the working fluids are aqueous solutions, their electrodes must be housed in open reservoirs of the side channels to allow release of the bubbles (Oddy et al. 2001).

### 3.2.4 AC electrokinetic instability mixing

As mentioned in DC EKI mixing, more chaotic flow patterns may be induced by time-dependent electric fields, which can improve the mixing performance at a low intensity of electric field. Oddy et al. (2001) first presented an active micromixer in which an AC electric field induces a more chaotic flow field to enhance the mixing of a two pressure-driven flow stream (conductivity ratio of two streams was not provided in their work). A high intensity AC electric field (1 kV/cm with a relatively low frequency) from side channels was still required to induce electrokinetic instability for enhancing mixing in their experiments. As shown in Fig. 17, the experimental results showed that the average velocity of the main flow stream is 0.5 mm/s, and the EKI flow field resulted in a rapid stretching and

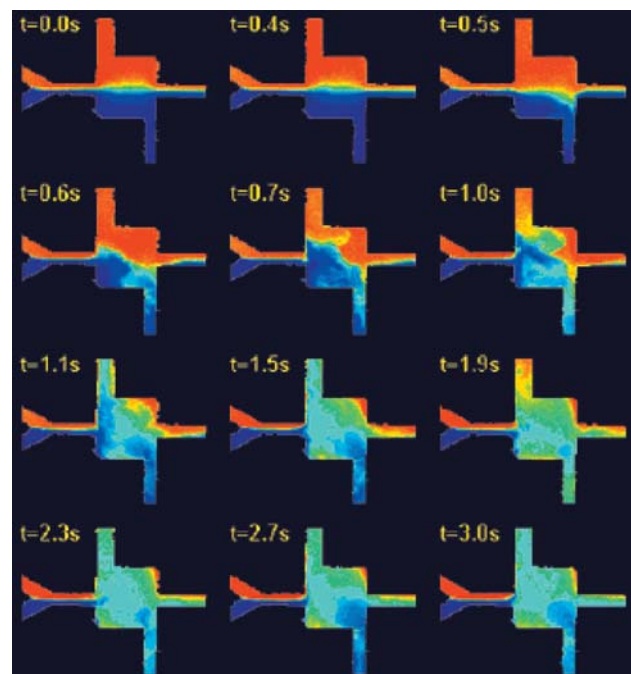


**Fig. 17** Experimental images of EKI mixing in a micro-chamber (Oddy et al. 2001)

folding of the fluid in the chamber and achieved an effective mixing performance within 3 s, corresponding to less than 1% of the time required to achieve mixing via diffusion effects in a conventional straight microchannel. In their experiments, no information was mentioned concerning whether time-dependent electric field could be used to improve EKI mixing performance. Nevertheless, it was demonstrated by Shin et al. (2005). In Fig. 18, it can be seen that the more chaotic trajectories can be generated in a cross-shaped microchannel by a time-dependent electric field. The dynamic voltage ( $V_{DC} + V_{AC} \sin(2\pi ft)$ ) is applied to inlet port II and a static voltage ( $V_{DC}$ ) is applied to inlet ports I and III. There is an optimal frequency ( $f$ ) of 12 Hz for enhancing the instability and fluid mixing in their studies.

### 3.2.5 Periodically switching electroosmotic mixing

An efficient active mixing scheme to enhance the mixing effect of two pressure-driven flow streams at low Reynolds number is performed by pulsing their velocities or pressures in some way; this has been investigated by many researchers (Niu and Lee 2003; Glasgow et al. 2004; Okkels and Tabeling 2004; Dodge et al. 2005). For example, Okkels and Tabeling (2004) and Dodge et al. (2005) presented a mixer comprising a main channel and one pair of

side channels in which the mixing species were stirred by pulsing the velocities of the fluids introduced through the side channels. This concept was also extended to a chaotic mixer comprising one main channel and multiple pairs of side channels (Niu and Lee 2003). The fluid elements in the main channel can be stretched and folded repeatedly and efficiently and then resulted in chaotic mixing when an appropriate amplitude and frequency of perturbation was applied. There are two important factors to achieve chaotic mixing in these systems in addition to applying an appropriate amplitude and frequency of perturbation. One is the corners at the intersection of the main and side channels which are locations for saddle points; another is that the velocity profile of pressure-driven flow is parabolic-like. In general, the stretching rate of the fluid element in pressure-driven flow fields is much larger than that in electroosmotic flow fields. This is because the electrical double layer is always much smaller than the microchannel dimension; this then results in a plug-like velocity profile. In other words, the efficient stretching and folding of the fluid element or chaotic mixing in pure electroosmotic flow fields may be difficult to be achieved by periodically switching an externally applied electric field in side channels. As shown in Fig. 19, it can be seen that the species distributions or interfaces for any switching frequency are all regular and smooth, and chaotic mixing cannot occur (Tang et al. 2002). This phenomenon was also observed numerically and experimentally (MacInnes 2002; Lin et al. 2004a). Nevertheless the mixing can also be enhanced by increasing the interfacial contact area to improve the efficiency of mass transfer based on molecular diffusion in a simple microchannel at an optimal switching frequency or Strouhal number (Lin et al. 2004a; Glasgow et al. 2004). This increased contact area still has a limited value, which is unlikely to produce chaotic mixing. Hence, this active electroosmotic mixing scheme is only suitable

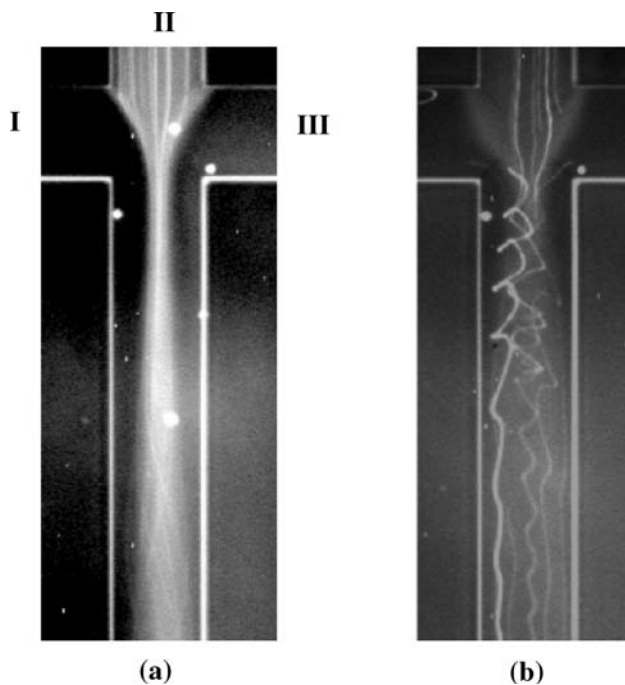


**Fig. 18** Fluorescent particle trajectories for different conditions of electric fields. **a** Static electric field with  $V_{DC} = 650$  V and **b** dynamic electric field with  $V_{DC} = 650$  V,  $V_{AC} = 50$  V and  $f = 12$  Hz. Here the intensity of electric field is approximately 300 V/cm and the conductivity ratio is 10 (Shin et al. 2005)

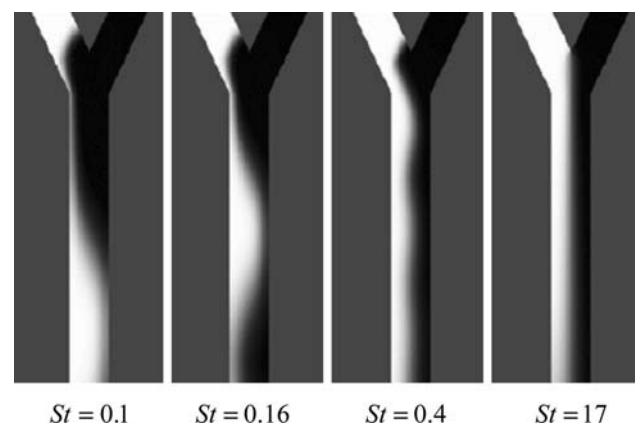


**Fig. 19** Species distributions in the periodically switching electroosmotic flow field for a Peclet number  $Pe = 500$  at different Strouhal numbers  $St = fW/U$  (Tang et al. 2002)



for enhancing species mixing at low Péclet number regimes. Fu et al. (2005) also used this scheme to improve the mixing performance of multiple (four) streams in a microchannel at low Peclet number regimes, as shown in Fig. 20. In general, the two species mixing streams may not be easily arranged to form mixing of sub-multiple parallel streams in in-plane microchannel structures. The arrangement of multiple streams only can be obtained artificially, e.g. the four streams with two species are injected separately from four inlet ports as shown in Fig. 20. Actually, this mixer is not conveniently integrated into microfluidic systems.

This concept was also extended to electroosmotic mixing through a sequential injection strategy (Coleman and Sinton 2005; Coleman et al. 2006). As shown in Fig. 21, the sample (fluorescent dye) from inlet port A is firstly dynamically loaded in a cross-shaped region and then dispensed to the downstream by the side flow from inlet port B. Repeating the above procedure periodically, the mixing is greatly enhanced by means of the reduced flow velocity, the reduced striation thickness (diffusion length scale), and the increased interfacial contact area in the mixing chamber; these all result from the expansion effect in a sudden expansion chamber. Without a sudden expansion chamber, the mixing may be poor using this mixing strategy. This is because the Taylor dispersion effect in electroosmotic flow is always not significant in a straight channel compared to that in pressure-driven flow (Nguyen and Huang 2005). Nevertheless, the sample band flows through a turn microchannel and would be spread due to the race-track effect and results in dispersion effect (Culbertson et al. 1998; Griffiths and Nilson 2000; Molho et al. 2001). Therefore, the samples can be stretched repeatedly in a twisted channel, which may be helpful in improving mixing in the sequential injection electroosmotic mixing scheme.

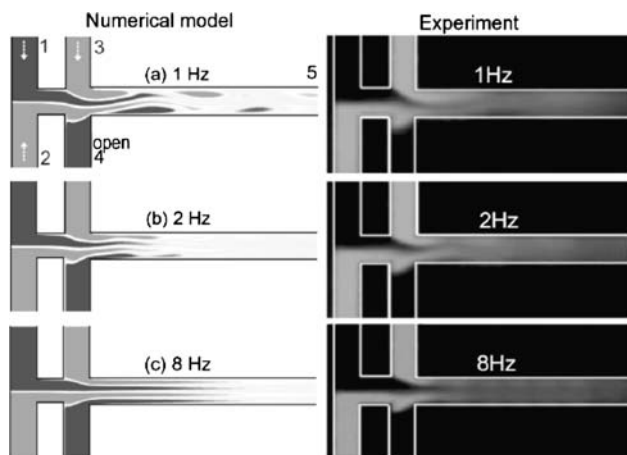


**Fig. 20** Periodically switching electroosmotic multiple stream mixing at an electric field of 100 V/cm for different switching frequencies (Fu et al. 2005)

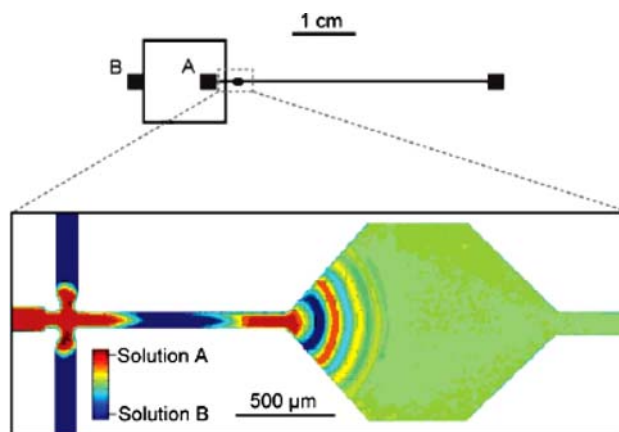


**Fig. 21** Electroosmotic sequential injection mixing (Coleman et al. 2006)

### 3.2.6 Field-induced electroosmosis enhanced mixing

Field-induced electroosmosis has been widely applied to the active control of electroosmotic flows (Schasfoort et al. 1999) and liquid pumping in microchannels (Ajdari 2000; Brown et al. 2001; Studer et al. 2002; Mpholo et al. 2003; Ramos et al. 2003; Lastochkin et al. 2004; Bazant and Ben 2006), with a lesser application in micromixing. Some examples of the application of field-induced electroosmosis for enhancing micromixing in the literature are introduced in the following sections.

*Field-effect induced non-uniform zeta potentials* In contrast to a passive mixer using non-uniform time-independent zeta potentials as mentioned previously, time-independent or dependent non-uniform zeta potentials can be controlled actively using a field-effect (i.e. the so-called capacitive effect) (Lee et al. 1991; Schasfoort et al. 1999). According to the three-capacitor model proposed by Lee et al. (1991), the field-effect induced zeta potential ( $\zeta_i$ ) can be expressed as

$$\zeta_i = \frac{C_{wall}}{C_{EDL}} V_a, \tag{10}$$

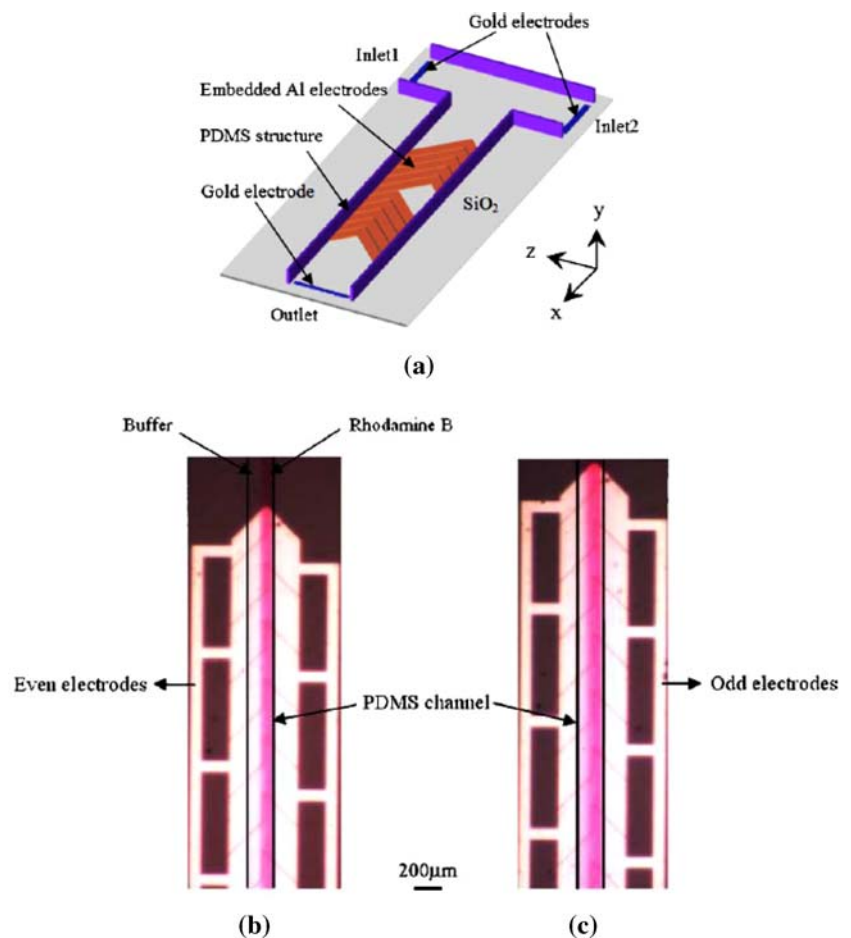
where  $V_a$  is the applied voltage on the electrode embedded beneath the solid-liquid interface and insulated from the liquid, and  $C_{wall}$  and  $C_{EDL}$  are the capacitance of the channel wall and the electrical double layer, respectively.  $C_{wall}$  is inversely proportional to the distance between the embedded electrode and the channel wall, implying that the magnitude of the induced zeta potential increases as the distance decreases at a constant applied voltage.  $C_{EDL}$  is dependent on the pH value and concentration of the electrolyte (Hunter 1981). A positive applied voltage induces a positive zeta potential, while a negative voltage induces a

negative zeta potential. In addition, there are two time scales should be considered for the cases of time-dependent induced zeta potentials. One is the charged time for the EDL capacitor ( $\lambda_D^2/D_i$ ,  $D_i$  is the diffusivity of ions in electrolyte), which is generally less than several microseconds when the EDL thickness is thin. Another is that the time required for fully charging the capacitor of the wall (i.e. RC time or charge relaxation time  $t_c = \epsilon_s/\sigma_s$ ,  $\epsilon_s$  and  $\sigma_s$  are the permittivity and conductivity of the channel substrate, respectively). For example, the charge relaxation time for the Pyrex 7740/soda-lime glass is on the order of  $10^{-2}$  s. Once the period of the time-switching applied voltage is much larger than the two charge relaxation time scales, the value of the time-dependent induced zeta potential can be regarded as  $\zeta_i$ . In general, the zeta potential of the channel wall ( $\zeta$ ) is represented as the sum of  $\zeta_i$  and  $\zeta_o$  (original zeta potential dominated by the permanent surface charge of the channel wall). When the induced zeta potential is much larger than the original zeta potential, the zeta potential of the channel wall can be represented as  $\zeta_i$ .

Wu and Liu (2005) used the field-effect approach to induce a non-uniform time-dependent zeta potential distribution in the bottom wall of the PDMS microchan-

nel, as shown in Fig. 22. Figure 22 (c) shows that the electroosmotic flow mixing is greatly enhanced by applying a 0.5 Hz, 100 V/–50 V square-wave voltage to the staggered asymmetric herringbone electrodes; the mixing efficiency achieves 90% after the fluids pass through a 5 mm long microchannel. In addition, Qian and Bau (2002) also used a field-effect to apply time-wise periodic alterations of the zeta potential along the two-dimensional microchannel walls to induce an electroosmotic chaotic advection effect in a closed flow system. Their designs also fit within the LTM framework (Ottino and Wiggins 2004b). In their study, they assumed the induced zeta potential is much larger than the original zeta potential. As such, the induced zeta potential dominates the zeta potential of the channel wall. As shown in Fig. 23, two electroosmotic flow patterns are induced in a closed system with two different zeta potential distributions. The effect of periodically switching between two flow fields at various periods was analyzed by performing particle tracking simulations (i.e. Poincaré maps). The results indicated that a more chaotic mixing effect was achieved at an appropriate value of the switching frequency (i.e.  $1/T$ ), as shown in Fig. 24. This concept also

**Fig. 22** a Schematic of a T-shaped electroosmotic mixing channel with a  $200\ \mu\text{m} \times 60\ \mu\text{m}$  cross-section. The embedded electrodes were arranged in a staggered asymmetric herringbone configuration. A  $5\ \mu\text{m}$  gap between the adjacent embedded electrodes was created. Experimental images of mixing under b zero applied voltage and c applied alternate 100 V/–50 V at odd/even embedded electrodes. The external electric field strength in the microchannel is 86 V/cm (Wu and Liu 2005)



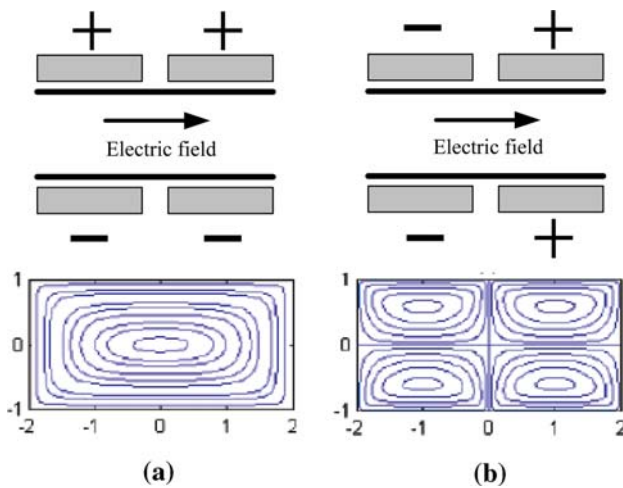


**Fig. 23** Flow patterns induced by two different zeta potential distributions in a closed flow system. The symbols “+” and “-” represent the positive and negative applied voltage at the embedded electrodes, respectively (Qian and Bau 2002)

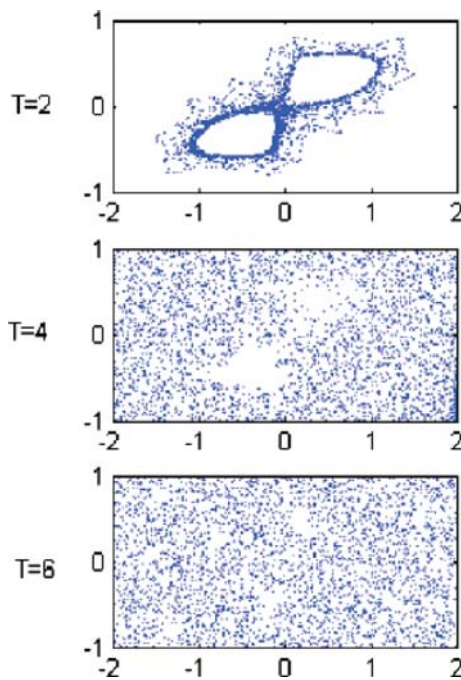


**Fig. 24** Poincaré maps for the periodically switching of two flow patterns as shown in Fig. 23 at various dimensionless periods  $T = 2, 4$  and  $6$  (Qian and Bau 2002)

extended to the mixing enhancement in open flow systems (i.e. continuous flow system) (Lee et al. 2004; Lin et al. 2005). Figure 25 shows that the particle trajectories are disturbed and the mixing is enhanced under applied alternate voltages (900 V) at inclined electrodes with a frequency 0.5 Hz. This applied voltage is too high for a viable microfluidic system and should be reduced by

decreasing the distance between the channel wall and the embedded electrodes to induce an effective zeta potential. Although mixing efficiency in their system is improved, the chaotic behavior is not significant.

*AC electroosmosis induced secondary flows* Sasaki et al. (2006) proposed a rapid micromixing scheme for a pressure-driven flow system combined with AC electroosmosis. AC electroosmosis can be induced by an AC field without electrochemical reactions on electrodes like electrolysis and bubble generation, so long as the frequency is higher than the inverse electrode reaction time ( $>1$  kHz). In general, the maximum AC electroosmotic effect occurs as the frequency approaches the inverse charging time scale (RC time) for forming a polarization double layer on the electrode surface (i.e.  $t_c \approx \lambda_D d / D_i$ , where  $d$  is the separation distance between a pair of electrodes). The double layer polarization is induced by a capacitive charging mechanism (Ajdari 2000; Green et al. 2000; Gonzalez et al. 2000). The time-averaged slip velocity on the electrode surface was derived by Gonzalez et al. 2000; this is proportional to the square of the applied voltage on electrode. Therefore, a higher electroosmotic flow velocity can be produced with a lower applied voltage at an optimal frequency. Figure 26a shows a schematic of an AC electroosmosis induced flow pattern in a microchannel with a semi-elliptic cross section. By designing a twisted electrode patterning configuration as shown in Fig. 26b, a blinking vortex flow can be produced in the downstream channel which results in a chaotic mixing. This mixer also fits within the LTM framework (Ottino and Wiggins 2004b). However, their results show that the channel length required for 90% mixing increases as the main stream velocity increases under a constant applied voltage and frequency. This is because the ratio of the transverse flow to streamwise flow component decreases as the main stream velocity increases, which results in a weaker secondary flow.

The electrokinetic micromixer described above is only suitable for pressure-driven flow systems and not electrokinetically driven flow systems. Furthermore, Lastochkin et al. (2004) also proposed an AC electroosmotic mixer for electrokinetically driven flow systems. In this system, high throughput liquid-pumping and mixing were both achieved through Faradic charging AC electroosmosis and specific arrangement of electrodes in microchannels. Faradic charging AC electroosmosis is induced by driving Faradic reactions on electrodes deliberately, which is different than the capacitive charging AC electroosmosis mentioned above. The magnitude of flow velocity depends exponentially on the applied voltage and achieves a stronger flow than that of capacitive charging AC electroosmosis under a lower applied voltage.

**Fig. 25 a** Photograph of a Y-shape mixing channel with the arrangement of inclined embedded electrodes.

Fluorescence images of **b** the particle trajectories and **c** the species mixing at different times. The external electric field strength in the microchannel is of 200 V/cm (Lin et al. 2005)

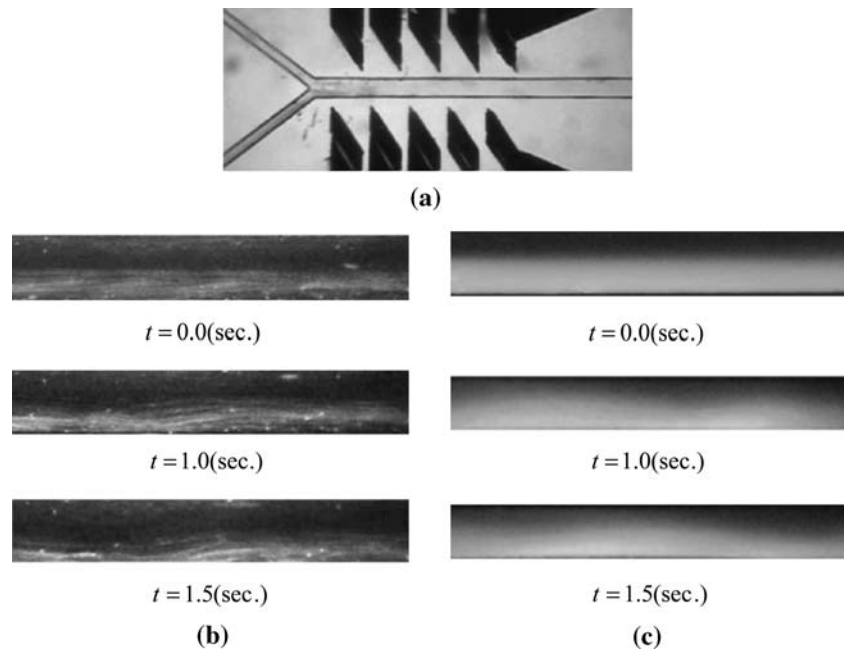
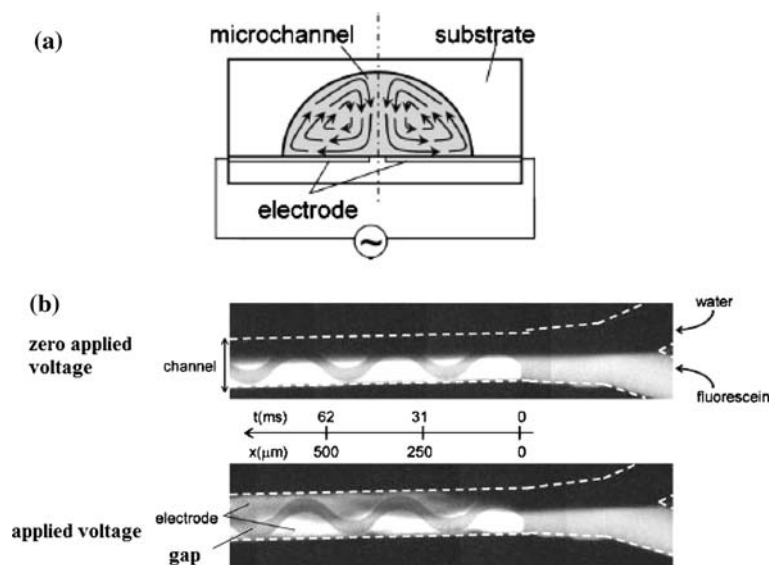


**Fig. 26 a** Schematic of AC electroosmosis induced a secondary flow in a microchannel with a pair of coplanar electrodes. **b** Fluorescence images of mixing between two streams with or without an applied sinusoidal voltage (20 V, 1 kHz). Mean axial velocity of main stream was 8.1 mm/s (Sasaki et al. 2006)

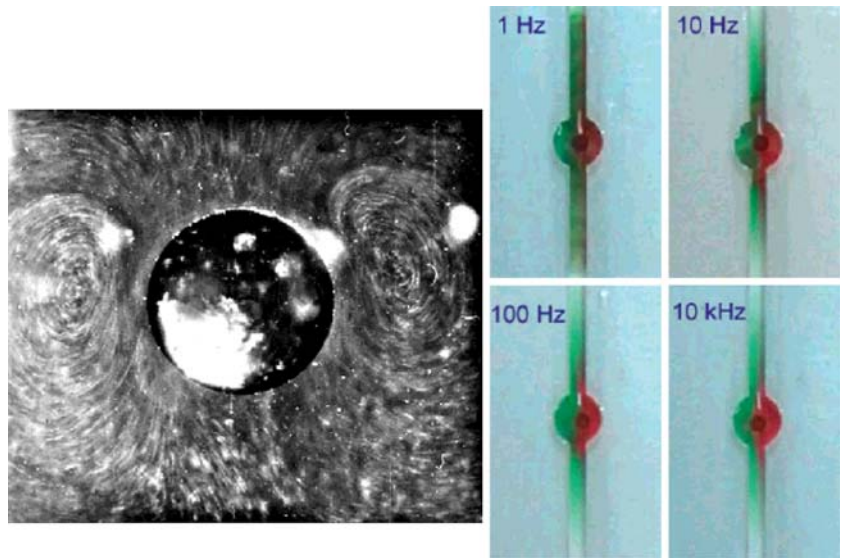


*Nonlinear electroosmotic vortices generated around a conducting ion-exchange granular or near a dielectric sharp corner*

As shown in Fig. 27a, a conducting ion-exchange granular is inserted into an electrolyte with a DC field, due to field penetration (electric field) across the conducting granular, whereas the streamlines do not penetrate the granular, the velocity field no longer coincides with the electric field and is hence no longer irrotational, and then an electroosmotic vortex pair is generated (Dukhin 1991; Mishchuk and Takhistov 1995; Ben and Chang 2002). This phenomenon is so-called electroosmosis of the

second kind (Dukhin 1991; Mishchuk and Takhistov 1995). According to Dukhin's theory, the effective zeta potential is estimated to be on the order  $Ea$ , where  $E$  and  $a$  are the external electric field and granular size, respectively. Therefore, the electroosmotic slip velocity is estimated to be proportional to the square of the external electric field. Hence, the induced vortex is also called a nonlinear electroosmotic vortex. The nonlinear electroosmotic vortices are closed under DC fields (see Fig. 27a) and may result in a poor mixing. As an example, AC field nonlinear electroosmotic vortices were applied to improve micromixing

**Fig. 27** **a** Experiment image of an electroosmotic vortex pair near a cation-exchange granular was generated under a DC field. **b** Nonlinear electroosmotic vortices mixing under AC fields (square waveform: 130 V/cm) with different frequencies (Wang et al. 2004)



in a closed flow system (Wang et al. 2004), as shown in Fig. 27b. The experimental images were captured at 30 s after the AC field was applied. Their results show that mixing is greatly enhanced at a lower frequency. The nonlinear electroosmotic vortices within this mixer can enhance micromixing in a closed system but are not suitable for an open flow system. In addition, it is difficult to be integrated in microfluidic systems because a conducting granular is required. Nevertheless, nonlinear electroosmotic vortices also can be obtained by patterning porous structures or surfaces in microchannels instead of a conducting granular.

Furthermore, due to field penetration across the dielectric sharp corner (note: the electric field strength near the corner is in excess of  $E_s \sim \zeta/\lambda_D$ ), electroosmotic vortices can also be induced near the dielectric corners (Thamida and Chang 2002; Yossifon 2006). Wang et al. (2006b) also used the electroosmotic vortices to enhance mixing in a four-corner chamber (3 mm diameter) under an AC field, as shown in Fig. 28. Their results show that a two-order reduction in mixing time can be achieved at a high frequency. Similarly, this mixer is not suitable for an open flow system. In an open flow system, we believe that the electroosmotic vortices can also be produced to enhance mixing by patterning periodic sharp corners along the mixing channel.

In general, there remain opportunities for new developments in electrokinetic micromixers based on field-induced electroosmosis. For example, nonlinear electroosmosis induced on metal surfaces has been applied for high throughput liquid pumping (Bazant and Ben 2006). In addition, it has also shows good potential for developing a novel electrokinetic micromixer in electrokinetically driven

microfluidic systems through a specific design (Bazant and Squires 2004).

#### 4 Conclusions and future directions

It seems likely that future micromixer designs will continue along the current trend for implementing species mixing without the use of moving mechanical parts. Furthermore, it seems reasonable to speculate that the use of electrokinetic forces to induce a mixing effect will become

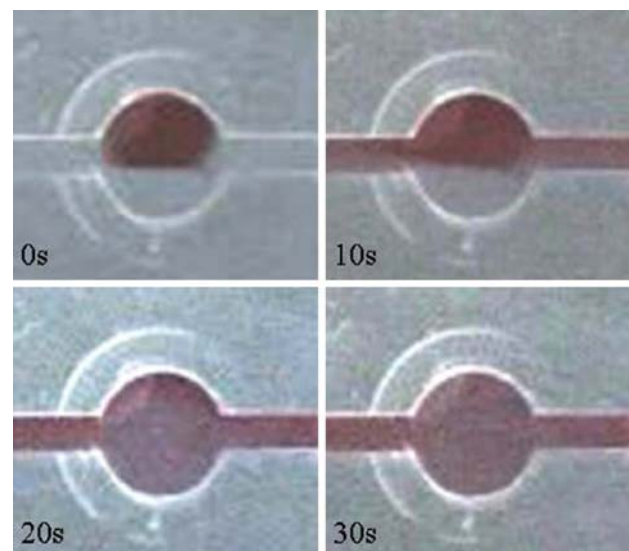


**Fig. 28** Experimental images of mixing in a chamber at different times by applying a sinusoidal AC field (94 V/cm, 100 kHz) (Wang et al. 2006b)

increasingly common since this technique greatly simplifies the microfabrication process and reduces the cost and complexity involved in embedding active or passive mixers within microfluidic systems. Electrokinetically driven flows in microfluidic devices are generally limited to low Reynolds number regimes and typically involve biomolecule transport with low molecular diffusivity. Hence, micromixers are obliged to function under conditions of low Reynolds numbers and high Péclet numbers. However, current diffusion-based micromixing schemes, e.g. parallel lamination mixing, provide only an acceptable mixing result at low Péclet numbers. In contrast, the performance of chaotic advection mixers is not largely dependent on the Péclet number. Accordingly, the development of future micromixers should focus particularly on passive or active chaotic mixing schemes (e.g. Johnson et al. 2002; Biddiss et al. 2004; Wu and Liu 2005; Shin et al. 2004; Park et al. 2005; Tai et al. 2006). However, current EKI-based chaotic mixers suffer the drawbacks of requiring high electrical voltages and electrical conductivity gradients. In DC electrokinetically driven microfluidic systems, high flow rates usually require high electric field strengths, and even then a high power supply is required. This is a great disadvantage in trying to realize a portable microfluidic system. Accordingly, low-voltage, AC electrokinetic techniques (field-induced electroosmosis) are expected to receive increasing attention in the coming years (Chang 2006). Finally, it is known that the high flow rates required to achieve species mixing can be produced through various nonlinear electrokinetic phenomena. Therefore, the application of nonlinear electrokinetic techniques to realize active mixers and portable microfluidic systems is likely to emerge as a major research topic in the microfluidics community in the near future.

## References

- Ajdari A (1995) Electro-osmosis on inhomogeneous charged surfaces. *Phys Rev Lett* 75:755–758
- Ajdari A (1996) Generation of transverse fluid currents and forces by an electric field: electro-osmosis on charge-modulated and undulate surfaces. *Phys Rev E* 53:4996–5005
- Ajdari A (2000) Pumping liquids using asymmetric electrode arrays. *Phys Rev E* 61:R45–R48
- Ajdari A (2001) Transverse electrokinetic and microfluidic effects in micropatterned channels: lubrication analysis for slab geometries. *Phys Rev E* 65:016301
- Anderson JL, Idol WK (1985) Electroosmosis through pores with nonuniformly charged walls. *Chem Eng Commun* 38:93–106
- Bazant MZ, Ben Y (2006) Theoretical prediction of fast 3D AC electro-osmotic pumps. *Lab Chip* 6:1455–1461
- Bazant MZ, Squires TM (2004) Induced-charge electrokinetic phenomena: theory and microfluidic applications. *Phys Rev Lett* 92:066101
- Ben Y, Chang H-C (2002) Nonlinear Smoluchowski slip velocity and micro-vortex generation. *J Fluid Mech* 461:229–238
- Biddiss E, Erickson D, Li D (2004) Heterogeneous surface charge enhanced micromixing for electrokinetic flows. *Anal Chem* 76:3208–3213
- Brown ABD, Smith CG, Rennie AR (2001) Pumping of water with AC electric fields applied to asymmetric pairs of microelectrodes. *Phys Rev E* 63: 016305
- Chang H-C (2006) Electro-kinetics: a viable micro-fluidic platform for miniature diagnostic kits. *Can J Chem Eng* 84:146–160
- Chang C-C, Yang R-J (2004) Computational analysis of electrokinetically driven flow mixing with patterned blocks. *J Micromech Microeng* 14: 550–558
- Chang C-C, Yang R-J (2006) A particle tracking method for analyzing chaotic electroosmotic flow mixing in 3-D microchannels with patterned charged surfaces. *J Micromech Microeng* 16:1453–1462
- Chang M-S, Homsy GM (2005) Effects of Joule heating on the stability of time-modulated electro-osmotic flow. *Phys Fluids* 17:074107
- Chen C-H, Lin H, Lele SK, Santiago JG (2005) Convective and absolute electrokinetic instability with conductivity gradients. *J Fluid Mech* 524:263–303
- Chen J-K, Luo W-J, Yang R-J (2006) Electroosmotic flow driven by DC and AC electric fields in curved microchannels. *Jap J Appl Phys* 45: 7983–7990
- Coleman JT, Sinton D (2005) A sequential injection microfluidic mixing strategy. *Microfluid Nanofluid* 1:319–327
- Coleman JT, Mckechnie J, Sinton D (2006) High-efficiency electrokinetic micromixing through symmetric sequential injection and expansion. *Lab Chip* 6:1033–1039
- Craighead H (2006) Future lab-on-a-chip technologies for interrogating individual molecules. *Nature* 442:387–393
- Culbertson CT, Jacobson SC, Ramsey JM (1998) Dispersion sources for compact geometries on microchips. *Anal Chem* 70:3781–3789
- Cummings EB, Griffiths SK, Nilson RH, Paul PH (2000) Conditions for similitude between the fluid velocity and electric field in electroosmotic flow. *Anal Chem* 72:2526–2532
- deMello AJ (2006) Control and detection of chemical reactions in microfluidic systems. *Nature* 442:394–402
- Deval J, Tabling P, Ho C-M (2002) A dielectrophoretic chaotic mixer. In: Proc 15th IEEE Workshop on MEMS, Las Vegas, USA, pp 36–39
- Dodge A, Hountondji A, Jullien MC, Tabeling P (2005) Spatiotemporal resonances in a microfluidic system. *Phys Rev E* 72:056312
- Dukhin SS (1991) Electrokinetic phenomena of the second kind and their application. *Adv Colloid Interf Sci* 35:173–196
- El-Ali J, Sorger PK, Jensen KF (2006) Cells on chips. *Nature* 442:403–411
- El Moctar AO, Aubry N, Batton J (2003) Electro-hydrodynamic micro-fluidic mixer. *Lab on a Chip* 3:273–280
- Erickson D, Li D (2002) Influence of surface heterogeneity on electrokinetically driven microfluidic mixing. *Langmuir* 18:1883–1892
- Erickson D, Li D (2003) Three-dimensional structure of electroosmotic flow over heterogeneous surfaces. *J Phys Chem* 107:12212–12220
- Fair RB (2007) Digital microfluidics: is a true lab-on-a-chip possible? *Microfluid. Nanofluid* 3:245–281
- Fushinobu K, Nakata M (2005) An experimental and numerical study of a liquid mixing device for Microsystems. *Trans ASME J Electronic Packaging* 127:141–146

- Fu L-M, Lin J-Y, Yang R-J (2003) Analysis of electroosmotic flow with step change in zeta potential. *J Colloid Interf Sci* 258:266–275
- Fu L-M, Yang R-J, Lin C-H, Chien Y-S (2005) A novel microfluidic mixer utilizing electrokinetic driving forces under low switching frequency. *Electrophoresis* 26:1814–1824
- Glasgow I, Lieber S, Aubry N (2004) Parameters influencing pulsed flow mixing in microchannels. *Anal Chem* 76:4825–4832
- Glasgow I, Batton J, Aubry N (2004) Electroosmotic mixing in microchannels. *Lab Chip* 4:558–562
- Gonzalez A, Ramos A, Green NG, Castellanos A, Morgan H (2000) Fluid flow induced by nonuniform AC electric fields in electrolytes on microelectrodes. II. A linear double layer analysis. *Phys Rev E* 61: 4019–4028
- Green NG, Ramos A, Gonzalez A, Morgan H, Castellanos A (2000) Fluid flow induced by nonuniform AC electric fields in electrolytes on microelectrodes. I. Experimental measurements. *Phys Rev E* 61: 4011–4018
- Griffiths SK, Nilson RH (2000) Band spreading in two-dimensional microchannel turns for electrokinetic species transport. *Anal Chem* 72: 5473–5482
- Hardt S, Drese K S, Hessel V, Schönfeld F (2005) Passive micromixers for applications in the microreactor and  $\mu$ TAS fields. *Microfluid Nanofluid* 1:108–118
- Hardt S, Pennemann H, Schönfeld F (2006) Theoretical and experimental characterization of a low-Reynolds number split-and-recombine mixer. *Microfluid. Nanofluid* 2:237–248
- Hardt S, Schönfeld F (2003) Laminar mixing in different interdigital micromixers: II. Numerical simulations. *AIChE J* 49:578–584
- Hau WLW, Trau DW, Sucher NJ, Wong M, Zohar Y (2003) Surface-chemistry technology for micro fluidics. *J Micromech Microeng* 13:272–278
- Herr AE, Molho JI, Santiago JG, Mungal MG, Kenny TW, Garguilo MG (2000) Electroosmotic capillary flow with nonuniform zeta potential. *Anal Chem* 72:1052–1057
- Hertzog DE, Michalet X, Jager M, Kong X, Santiago JG, Weiss S, Bakajin O (2004) Femtomole mixer for microsecond kinetic studies of protein folding. *Anal Chem* 76:7169–7178
- Hessel V, Löwe H, Schönfeld F (2005) Micromixers—a review on passive and active mixing principles. *Chem Eng Sci* 60:2479–2501
- Hessel V, Hardt S, Löwe H, Schönfeld F (2003) Laminar mixing in different interdigital micromixers: I. Experimental characterization. *AIChE J* 49:566–577
- Hoburg JF, Melcher JR (1976) Internal electrohydrodynamic instability and mixing of fluids with orthogonal field and conductivity gradients. *J Fluid Mech* 73:333–351
- Hoburg JF, Melcher JR (1977) Electrohydrodynamic mixing and instability induced by colinear fields and conductivity gradients. *Phys Fluids* 20: 903–911
- Huang M-Z, Yang R-J, Tai C-H, Tsai C-H, Fu L-M (2006) Application of electrokinetic instability flow for enhanced micromixing in cross-shaped microchannel. *Biomed Microdevices* 8:309–315
- Hunter RJ (1981) *Zeta potential in colloid science: principles and applications*. Academic, New York
- Ismagilov RF, Stroock AD, Kenis PJA, Whitesides GM, Stone HA (2000) Experimental and theoretical scaling laws for transverse diffusive broadening in two-phase laminar flow in microchannels. *Appl Phys Lett* 76:2376–2378
- Jacobson SC, McKnight TE, Ramsey JM (1999) Microfluidic devices for electrokinetically driven parallel and serial mixing. *Anal Chem* 71:4455–4459
- Jacobson SC, Ramsey JM (1997) Electrokinetic focusing in microfabricated channel structures. *Anal Chem* 69:3212–3217
- Janasek D, Franzke J, Manz A (2006) Scaling and the design of miniaturized chemical-analysis systems. *Nature* 442:374–380
- Johnson TJ, Ross D, Locascio LE (2002) Rapid microfluidic mixing. *Anal Chem* 74:45–51
- Johnson TJ, Locascio LE (2002) Characterization of optimization of slanted well design for microfluidic mixing under electroosmotic flow. *Lab Chip* 2:135–140
- Jones TB (2005) *Electromechanics of particles*. Cambridge University Press, Cambridge
- Kamholz AE, Weigl BH, Finlayson BA, Yager P (1999) Quantitative analysis of molecular interactive in microfluidic channel: the T-sensor. *Anal Chem* 71:5340–5347
- Knight JB, Vishwanath A, Brody JP, Austin RH (1998) Hydrodynamic focusing on a silicon chip: mixing nanoliters in micro-seconds. *Phys Rev Lett* 80:3863–3866
- Kohlheyer D, Besselink GAJ, Lammertink RGH, Schlautmann S, Unnikrishnan S, Schasfoort RBM (2005) Electro-osmotically controllable multi-flow microreactor. *Microfluid Nanofluid* 1:242–248
- Krishnamoorthy S, Feng J, Henry AC, Locascio LE, Hickman JJ, Sundaram S (2006) Simulation and experimental characterization of electroosmotic flow in surface modified channels. *Microfluid Nanofluid* 2:345–355
- Lastochkin D, Zhou R, Wang P, Ben Y, Chang H-C (2004) Electrokinetic micropump and micromixer design based on ac faradic polarization. *J Appl Phys* 96:1730–1733
- Lee CS, McManigill D, Wu CT, Patel B (1991) Factors affecting direct control of electroosmosis using an external electric field in capillary electrophoresis. *Anal Chem* 63:1519–1523
- Lee C-Y, Lee G-B, Fu L-M, Lee K-H, Yang R-J (2004) Electrokinetically driven active micro-mixers utilizing zeta potential variation induced by field effect. *J Micromech Microeng* 14:1392–1398
- Lee J, Moon H, Fowler J, Schoellhammer T, Kim C-J (2002) Electrowetting and electrowetting-on-dielectric for microscale liquid handling. *Sens Actuators A* 95:259–268
- Lee Y-K, Deval J, Tabling P, Ho C-M (2001) Chaotic mixing in electrokinetically and pressure driven micro flows. In: *Proc 14th IEEE Workshop on MEMS, Interlaken, Switzerland*, pp 483–486
- Li D (2004) *Electrokinetics in microfluidics*. Elsevier Academic Press
- Lin C-H, Fu L-M, Chien Y-S (2004a) Microfluidic T-form mixer utilizing switching electroosmotic flow. *Anal Chem* 76:5265–5272
- Lin H, Storey BD, Oddy MH, Chen C-H, Santiago JG (2004b) Instability of electrokinetic microchannel flows with conductivity gradients. *Phys Fluids* 16:1922–1935
- Lin J-L, Lee K-H, Lee G-B (2005) Active mixing inside microchannels utilizing dynamic variation of gradient zeta potentials. *Electrophoresis* 26:4605–4615
- Lin JZ, Zhang K, Li H-J (2006) Study on the mixing of fluid in curved microchannels with heterogeneous surface potentials. *Chin Phys* 15: 2688–2696
- Liu Y, Fanguy JC, Bledsoe JM, Henry CS (2000) Dynamic coating using polyelectrolyte multilayers for chemical control of electroosmotic flow in capillary electrophoresis microchips. *Anal Chem* 72:5939–5944
- Löb P, Drese KS, Hessel V, Hardt S, Hofmann C, Löwe H, Schenk R, Schönfeld F, Werner B (2004) Steering of liquid mixing speed in interdigital micro mixers—from very fast to deliberately slow mixing. *Chem Eng Technol* 27:340–345
- MacInnes JM (2002) Computation of reacting electrokinetic flow in microchannel geometries. *Chem Eng Sci* 57:4539–4558
- Mishchuk NA, Takhistov PV (1995) Electroosmosis of the second kind. *Colloids. Surf A* 95:119–131

- Molho JJ, Herr AE, Mosier B, Santiago JG, Kenny TW, Brennen RA, Gordon GB, Mohammadi (2001) Optimization of turn geometries for microchip electrophoresis. *Anal Chem* 73:1350–1360
- Moon H, Cho SK, Garrell RL, Kim C-J (2002) Low voltage electrowetting-on-dielectric. *J Appl Phys* 92:4080–4087
- Morgan H, Green NG (2003) *AC electrokinetics: colloids and nanoparticles*. Research Studies Press
- Mpholo M, Smith CG, Brown ABD (2003) Low voltage plug flow pumping using anisotropic electrode arrays. *Sens Actuators B* 92:262–268
- Ng ASW, Hau WLW, Lee Y-K, Zohar Y (2004) Electrokinetic generation of microvortex patterns in a microchannel liquid flow. *J Micromech Microeng* 14:247–255
- Nguyen N-T, Wu Z (2005) Micromixers—a review. *J Micromech Microeng* 15:R1–16
- Nguyen N-T, Huang X (2005) An analytical model for mixing based on time-interleaved sequential segmentation. *Microfluid Nanofluid* 1:373–375
- Niu X, Lee Y-K (2003) Efficient spatial-temporal chaotic mixing in microchannels. *J Micromech Microeng* 13:454–462
- Oddy MH, Santiago JG, Mikkelsen JC (2001) Electrokinetic instability micromixing. *Anal Chem* 73:5822–5832
- Okkels F, Tabeling P (2004) Spatiotemporal resonances in mixing of open viscous fluids. *Phys Rev Lett* 92:038301
- Ottino JM (1989) *The kinematics of mixing: stretching, chaos, and transport*. Cambridge University Press, Cambridge
- Ottino JM, Wiggins S (2004a) Introduction: mixing in microfluidics. *Phil Trans R Soc Lond A* 362:923–935
- Ottino JM, Wiggins S (2004b) Designing optimal micromixers. *Science* 305:485–486
- Paik P, Pamula VK, Pollack MG, Fair RB (2003a) Electrowetting-based droplet mixers for microfluidic systems. *Lab Chip* 3:28–33
- Paik P, Pamula VK, Fair RB (2003b) Rapid droplet mixers for digital microfluidic systems. *Lab Chip* 3:253–259
- Park J, Shin SM, Huh KY, Kang IS (2005) Application of electrokinetic instability for enhanced mixing in various micro-T-channel geometries. *Phys Fluids* 17:118101
- Pollack L, Tate MW, Darnton NC, Knight JB, Gruner SM, Eaton WA, Austin RH (1999) Compactness of the denatured state of a fast-folding protein measured by submillisecond small-angle X-ray scattering. *Proc Natl Acad Sci USA* 96:10115–10117
- Posner JD, Santiago JG (2006) Convective instability of electrokinetic flows in a cross-shaped microchannel. *J Fluid Mech* 555:1–42
- Probstein RF (1994) *Physicochemical hydrodynamics: an introduction*. Wiley–Interscience, New York
- Psaltis D, Quake SR, Yang C (2006) Developing optofluidic technology through the fusion of microfluidics and optics. *Nature* 442:381–386
- Qian S, Bau HH (2002) A chaotic electroosmotic stirrer. *Anal Chem* 74: 3616–3625
- Ramos A, Gonzalez A, Castellanos A, Green NG, Morgan H (2003) Pumping of liquids with AC voltages applied to asymmetric pairs of microelectrodes *Phys Rev E* 67:056302
- Ramos A, Morgan H, Green NG, Castellanos A (1999) AC electric-field-induced fluid flow in microelectrodes. *J Colloid Interf Sci* 217:420–422
- Ren L, Li D (2001) Electroosmotic flow in heterogeneous microchannels. *J Colloid Interf Sci* 243:255–261
- Sasaki N, Kitamori T, Kim H-B (2006) AC electroosmotic micromixer for chemical processing in a microchannel. *Lab Chip* 6:550–554
- Saville DA (1997) Electrohydrodynamics: the Taylor–Melcher leaky dielectric model. *Annu Rev Fluid Mech* 29:27–64
- Schasfoort RBM, Schlautmann S, Hendrikse J, Van den Berg A (1999) Field-effect flow control for microfabricated fluidic network. *Science* 286:942–945
- Schönfeld F, Hessel V, Hofmann C (2004) An optimised split-and-recombine micro-mixer with uniform ‘chaotic’ mixing. *Lab Chip* 4:65–69
- Shin SM, Kang IS, Cho Y-K (2005) Mixing enhancement by using electrokinetic instability under time-periodic electric field. *J Micromech Microeng* 15:455–462
- Sinton D (2004) Microscale flow visualization. *Microfluid Nanofluid* 1:2–21
- Song H, Bringer MR, Tice JD, Gerds C J, Ismagilov RF (2003) Experimental test of scaling of mixing by chaotic advection in droplets moving through microfluidic. *Appl Phys Lett* 83:4664–4666
- Sprott JC (2003) *Chaos and time-series analysis*. Oxford University Press, Oxford
- Squires TM, Bazant MZ (2004) Induced-charge electroosmosis. *J Fluid Mech* 509:217–252
- Squires TM, Quakes SR (2005) Microfluidics: fluid physics at the nanoliter scale. *Rev Mod Phys* 77:977–1026
- Stone HA, Stroock AD, Ajdari A (2004) Engineering flows in small devices: microfluidics toward a lab-on-a-chip. *Annu Rev Fluid Mech* 36:381–411
- Stroock AD, Dertinger SKW, Ajdari A, Mezic I, Stone HA, Whitesides GM (2002a) Chaotic mixer for microchannels. *Science* 295:647–651
- Stroock AD, Dertinger SKW, Whitesides GM, Ajdari A (2002b) Patterning flows using grooved surfaces. *Anal Chem* 74:5306–5312
- Stroock AD, Weck M, Chiu DT, Huck WTS, Kenis PJA, Ismagilov RF, Whitesides GM (2000) Patterning electro-osmotic flow with patterned surface charge. *Phys Rev Lett* 84:3314–3317
- Stroock AD, Whitesides GM (2003) Controlling flows in microchannels with patterned surface charge and topography. *Acc Chem Res* 36:597–604
- Studer V, Pepin A, Chen Y, Ajdari A (2002) Fabrication of microfluidic devices for AC electrokinetic fluid pumping. *Microelec Eng* 61–2: 915–920
- Succi S (2001) *The lattice Boltzmann equation: for fluid dynamics and beyond*. Oxford University Press, Oxford
- Suresh V, Homsy GM (2004) Stability of time-modulated electroosmotic flow. *Phys Fluids* 16:2349–2356
- Suzuki H, Ho C-M, Kasagi N (2004) A chaotic mixer for magnetic bead-based micro cell sorter. *J Microelectromech Syst* 13:779–790
- Tai C-H, Yang R-J, Huang M-Z, Liu C-W, Tsai C-H, Fu L-M (2006) Micromixer utilizing electrokinetic instability-induced shedding effect. *Electrophoresis* 27:4982–4990
- Tang GH, Li Z, Wang JK, He YL, Tao WQ (2006) Electroosmotic flow mixing in microchannels with the lattice Boltzmann method. *J Appl Phys* 100:094908
- Tang Z, Hong S, Djukic D, Modi V, West AC, Yardley J, Osgood RM (2002) Electrokinetic flow control for composition modulation in a microchannel. *J Micromech Microeng* 12:870–877
- Thamida SK, Chang, H-C (2002) Nonlinear electrokinetic ejection and entrainment due to polarization at nearly insulated wedges. *Phys Fluids* 14:4315–4328
- Tian F, Li B, Kwok DY (2005) Tradeoff between mixing and transport for electroosmotic flow in heterogeneous microchannels with nonuniform surface potentials. *Langmuir* 21:1126–1131
- Wang JK, Wang M, Li ZX (2005a) Lattice Boltzmann simulations of mixing enhancement by the electroosmotic flow in microchannels. *Mod Phys Lett B* 19:1515–1518



- Wang JK, Wang M, Li ZX (2006a) Lattice Poisson–Boltzmann simulations of electro-osmotic flows in microchannels. *J Colloid Interf Sci* 296:729–736
- Wang S-C, Chen H-P, Lee C-Y, Yu C-C, Chang H-C (2006b) AC electro-osmotic mixing induced by non-contact external electrodes. *Biosens Bioelectron* 22:563–567
- Wang S-C, Lai Y-W, Ben Y, Chang H-C (2004) Microfluidic mixing by dc and ac nonlinear electrokinetic vortex flows. *Ind Eng Chem Res* 43:2902–2911
- Wang Y, Lin Q, Mukherjee T (2005b) A model for laminar diffusion-based complex electrokinetic passive micromixers. *Lab Chip* 5:877–887
- Whitesides GM (2006) The origins and the future of microfluidics. *Nature* 442:368–373
- Wiggins S, Ottino JM (2004) Foundations of chaotic mixing. *Phil Trans R Soc Lond A* 362:937–970
- Wolf A, Swift JB, Swinney HL, Vastano J A (1985) Determining Lyapunov exponents from a time series. *Physica D* 16:285–317
- Wu C-H, Yang R-J (2006) Improving the mixing performance of side channel type micromixers using an optimal voltage control model. *Biomed Microdevices* 8:119–131
- Wu H-Y, Liu C-H (2005) A novel electrokinetic mixer. *Sens Actuators A* 118:107–115
- Yager P, Edwards T, Fu E, Helton K, Nelson K, Tam MR, Weigl BH (2006) Microfluidic diagnostic technologies for global public health. *Nature* 442(7101):412–418
- Yang R-J, Chang C-C (2004) Enhancement of electrokinetically-driven flow mixing in 3-D microchannels using heterogeneous surfaces. *IMECE'04: Anaheim, California, USA, IMECE2004-61441*
- Yang R-J, Chang C-C, Huang S-B, Lee G-B (2005) A new focusing model and switching approach for electrokinetic flow inside microchannels. *J Micromech Microeng* 15:2141–2148
- Yossifon G, Frankel I, Miloh T (2006) On electro-osmotic flows through microchannel junctions. *Phys Fluids* 18:117108